Discussion

Here we demonstrate that FGF-21 promotes engraftment of islet transplants. Only 3-day treatment with FGF-21 resulted in more insulin content in the islet grafts on day 30 compared to that in untreated mice. As previously reported, insulin content is correlated not only with islet mass but also with the function of pancreatic β-cells.[22] Indeed, our data on day 30 show that the better the blood glucose level, the more insulin content in the islet grafts (**Fig. 4B**). Because the first several days after transplantation are known to be the most critical period for engraftment of islet transplants, 3-day treatment of FGF-21 was most likely to be responsible for the suppression of islet graft loss.

Regarding the mechanism of action, FGF-21 has been reported to improve insulin sensitivity in adipose tissue and in liver by upregulating glucose uptake and by inhibition of glucose production, respectively,[14,23] and has been shown acute glucose-lowering action even by a single injection.[24] In this study, the mean blood glucose level in normoglycemic IT(+)/FGF(+) mice was already significantly decreased compared to that in IT(+)/FGF(-) mice (15.0 ± 4.7 vs. 31.6 ± 1.1 (mM), $p < 0.01$) on day 3 (**Fig. 1**). Unfortunately, insulin levels during IPGTT were too low for comparison even by using a highly sensitive insulin assay kit. However, the decrease in blood glucose levels despite the similar insulin content (**Fig. 4B**) suggests that FGF-21 treatment increased insulin sensitivity, which might well decrease the β-cell load and rescue β-cells from apoptosis, as has previously been reported.[25-27] On the other hand, as FGF-21 treatment has been found to have a direct cytoprotective effect on pancreatic β-cells,[15] FGF-21 might well similarly affect the graft in our transplantation model. We attempted to examine this immunohistologically, but it was not possible to find statistical difference because only 80 islets were transplanted in our experiment.

Our results also reveal lower body weight in FGF-21-treated mice than that in untreated mice on day 3. A noteworthy advantage of FGF-21 use is that it does not elicit adverse effects such as hypoglycemia and weight gain,[15] which often result from insulin use. Many agents have been reported to be beneficial for islet transplantation,[27-29] but unlike FGF-21, only a few are conducive to a broad spectrum of beneficial effects such as increased β-cell survival, insulin secretion and insulin synthesis, as well as indirectly reducing β-cell load via increased insulin sensitivity. Furthermore, FGF-21 is free of proliferative and tumorgenic effects,[14,15,30] which are major problems with most growth factors.

Because the half-life of FGF-21 is about 1 h when subcutaneously injected in mice,[16,24] we administered FGF-21 twice a day. Only 3-day administration resulted in better glycemic control, suggesting that more frequent or continuous administration of FGF-21 for a longer period might achieve even better glycemic control without body weight gain or hypoglycemia. For more effective usage in a clinical setting, a controlled-release type of FGF-21 might be developed.

In conclusion, clinical use of FGF-21 has the potential to improve engraftment results in islet transplantation, although further studies, especially in human, must be performed to clarify its therapeutic potential.

Materials and Methods

Animal care. All experiments were approved by the Kyoto University Animal Care Committee.

Animals. Male C57BL/6JJcl mice (CREA, Japan) aged 9–13 weeks were used as donors and those aged 7–9 weeks were used as recipients. Recipient animals were rendered diabetic by a single intraperitoneal injection (i.p.) of streptozotocin (STZ) (Sigma-Aldrich, USA), 120 mg/kg body weight, freshly dissolved in 100 mM citrate buffer (pH 4.2). Mice with blood glucose concentration greater than 20 mM for 2 days were used as recipients. Blood glucose concentrations were determined by glucose meter (Glucocard, Arkley, Japan).

Islet isolation, islet transplantation and FGF-21 treatment. Under anesthesia, 2 ml of Hanks balanced salt solution (HBSS) containing 1 mg collagenase was injected into the common bile duct of the donor mouse. The distended pancreas was removed and incubated at 37°C for 21 min. Islets were purified by Ficoll-density centrifugation and 80 freshly isolated islets were transplanted into the left sub-renal capsule of the anesthetized recipient mouse. Human FGF-21 (BioVendor Laboratory Medicine, Ins. Czech Republic) was administered to the mice (1.67 mg/kg body weight/day) twice daily for three days.

Glucose tolerance test. On day 30, the mice were fasted for 16 h, blood samples were collected at 0, 30, 60, 90 and 120 min after glucose injection (1.0 g/kg body weight, i.p.), and blood glucose levels were measured.

Insulin content and immunohistochemistry. The renal capsule of the kidney containing the islet graft was removed on day 3 and day 30 for measurement of insulin content and immunohistochemical analysis, respectively. Renal capsules were frozen in 4 mM of 4-(2-hydroxyethyl)-1-piperazineethanesulfonic acid (HEPES), then thawed and homogenized by ultrasonic waves and insulin levels were measured by radioimmunoassay (RIA). Kidneys were fixed overnight in 4% paraformaldehyde and transferred into 70% ethanol before processing through paraffin. Rabbit anti-insulin antibody (sc-9168, 1:100, Santa Cruz Biotechnology Inc., Santa Cruz, USA) and HRP-Labeled anti-Rabbit antibody (Dako Cytomation EnVision + System, Denmark) were used to detect insulin as primary and secondary antibody, respectively.

Statistical analyses. All data are presented as mean ± SE. Statistical analyses were performed by unpaired t-test and the Spearman rank correlation was used to assess correlation between the data. p value of less than 0.05 was considered significant.

Acknowledgements

This work was supported by a Research Grant on Nanotechnical Medicine from the Ministry of Health, Labour and Welfare of Japan, and by Scientific Research Grants from the Ministry of Education, Culture, Sports, Science and Technology of Japan, and also by Kyoto University Global COE Program "Center for Frontier Medicine."

References

1. Ornitz DM, Itoh N. Fibroblast growth factors. Genome Biol 2001; 2:3005.
2. Eswarakumar VP, Lax I, Schlessinger J. Cellular signaling by fibroblast growth factor receptors. Cytokine Growth Factor Rev 2005; 16:139-49.
3. Grose R, Dickson C. Fibroblast growth factor signaling in tumorigenesis. Cytokine Growth Factor Rev 2005; 16:179-86.
4. Presta M, Dell'Era P, Mitola S, Moroni E, Ronca R, Rusnati M. Fibroblast growth factor/fibroblast growth factor receptor system in angiogenesis. Cytokine Growth Factor Rev 2005; 16:159-78.
5. Itoh N, Ornitz DM. Evolution of the Fgf and Fgfr gene families. Trends Genet 2004; 20:563-9.
6. Hart AW, Baeza N, Apelqvist A, Edlund H. Attenuation of FGF signalling in mouse betacells leads to diabetes. Nature 2000; 408:864-8.
7. Revest JM, Spencer-Dene B, Kerr K, De Moerlooze L, Rosewell I, Dickson C. Fibroblast growth factor receptor 2-IIIb acts upstream of Shh and Fgf4 and is required for limb bud maintenance but not for the induction of Fgf8, Fgf10, Msx1 or Bmp4. Dev Biol 2001; 231:47-62.
8. Celli G, LaRochelle WJ, Mackem S, Sharp R, Merlino G. Soluble dominant-negative receptor uncovers essential roles for fibroblast growth factors in multi-organ induction and patterning. EMBO J 1998; 17:1642-55.
9. Elghazi L, Cras-Meneur C, Czernichow P, Scharfmann R. Role for FGFR2IIIb-mediated signals in controlling pancreatic endocrine progenitor cell proliferation. Proc Natl Acad Sci USA 2002; 99:3884-9.
10. Nishimura T, Nakatake Y, Konishi M, Itoh N. Identification of a novel FGF, FGF-21, preferentially expressed in the liver. Biochim Biophys Acta 2000; 1492:203-6.
11. Itoh N. The Fgf families in humans, mice and zebrafish: their evolutional processes and roles in development, metabolism and disease. Biol Pharm Bull 2007; 30:1819-25.
12. Kurosu H, Choi M, Ogawa Y, Dickson AS, Goetz R, Eliseenkova AV, et al. Tissue-specific expression of betaKlotho and fibroblast growth factor (FGF) receptor isoforms determines metabolic activity of FGF19 and FGF21. J Biol Chem 2007; 282:26687-95.
13. Ogawa Y, Kurosu H, Yamamoto M, Nandi A, Rosenblatt KP, Goetz R, et al. BetaKlotho is required for metabolic activity of fibroblast growth factor 21. Proc Natl Acad Sci USA 2007; 104:7432-7.
14. Kharitonenkov A, Shiyanova TL, Koester A, Ford AM, Micanovic R, Galbreath EJ, et al. FGF-21 as a novel metabolic regulator. J Clin Invest 2005; 115:1627-35.
15. Wente W, Efanov AM, Brenner M, Kharitonenkov A, Koster A, Sandusky GE, et al. Fibroblast growth factor-21 improves pancreatic beta-cell function and survival by activation of extracellular signal-regulated kinase 1/2 and Akt signaling pathways. Diabetes 2006; 55:2470-8.
16. Kharitonenkov A, Wroblewski VJ, Koester A, Chen YF, Clutinger CK, Tigno XT, et al. The metabolic state of diabetic monkeys is regulated by fibroblast growth factor-21. Endocrinology 2007; 148:774-81.
17. Shapiro AM, Lakey JR, Ryan EA, Korbutt GS, Toth E, Warnock GL, et al. Islet transplantation in seven patients with type 1 diabetes mellitus using a glucocorticoid-free immunosuppressive regimen. N Engl J Med 2000; 343:230-8.
18. Eich T, Eriksson O, Lundgren T. Visualization of early engraftment in clinical islet transplantation by positron-emission tomography. N Engl J Med 2007; 356:2754-5.
19. Barshes NR, Wyllie S, Goss JA. Inflammation-mediated dysfunction and apoptosis in pancreatic islet transplantation: implications for intrahepatic grafts. J Leukoc Biol 2005; 77:587-97.
20. Ryan EA, Paty BW, Senior PA, Bigam D, Alfadhli E, Kneteman NM, et al. Five-year follow-up after clinical islet transplantation. Diabetes 2005; 54:2060-9.
21. Yonekawa Y, Okitsu T, Wake K, Iwanaga Y, Noguchi H, Nagata H, et al. A new mouse model for intraportal islet transplantation with limited hepatic lobe as a graft site. Transplantation 2006; 82:712-5.
22. McCulloch DK, Koerker DJ, Kahn SE, Bonner-Weir S, Palmer JP. Correlations of in vivo beta-cell function tests with beta-cell mass and pancreatic insulin content in streptozocinadministered baboons. Diabetes 1991; 40:673-9.
23. Xu J, Lloid DJ, Hale C, Stanislaus S, Chen M, Sivits G, et al. Fibroblast growth factor 21 reverses hepatic steatosis, increases energy expenditure, and improves insulin sensitivity in diet-induced obese mice. Diabetes 2009; 58:250-9.
24. Xu J, Stanislaus S, Chinookoswong N, Lau YY, Hager T, Patel J, et al. Acute glucose-lowering and insulin-sensitizing action of FGF21 in insulin resistant mouse models—Association with liver and adipose tissue effects. Am J Physiol Endocrinol Metab 2009; 297: 1105-14.
25. Biarnes M, Montolio M, Nacher V, Raurell M, Soler J, Montanya E. Beta-cell death and mass in syngeneically transplanted islets exposed to short- and long-term hyperglycemia. Diabetes 2002; 51:66-72.
26. Merino JF, Nacher V, Raurell M, Aranda O, Soler J, Montanya E. Improved outcome of islet transplantation in insulin-treated diabetic mice: effects on beta-cell mass and function. Diabetologia 1997; 40:1004-10.
27. King A, Lock J, Xu G, Bonner-Weir S, Weir GC. Islet transplantation outcomes in mice are better with fresh islets and exendin-4 treatment. Diabetologia 2005; 48:2074-9.
28. Toyoda K, Okitsu T, Yamane S, Uonaga T, Liu X, Harada N, et al. GLP-1 receptor signaling protects pancreatic beta cells in intraportal islet transplant by inhibiting apoptosis. Biochem Biophys Res Commun 2008; 367:793-8.
29. Contreras JL, Eckstein C, Smyth CA, Bilbao G, Vilatoba M, Ringland SE, et al. Activated protein C preserves functional islet mass after intraportal transplantation: a novel link between endothelial cell activation, thrombosis, inflammation and islet cell death. Diabetes 2004; 53:2804-14.
30. Huang X, Yu C, Jin C, Yang C, Xie R, Cao D, et al. Forced expression of hepatocyte-specific fibroblast growth factor 21 delays initiation of chemically induced hepatocarcinogenesis. Mol Carcinog 2006; 45:934-42.

Exendin-4 Suppresses Src Activation and Reactive Oxygen Species Production in Diabetic Goto-Kakizaki Rat Islets in an Epac-Dependent Manner

Eri Mukai,[1,2] Shimpei Fujimoto,[1] Hiroki Sato,[1] Chitose Oneyama,[3] Rieko Kominato,[1] Yuichi Sato,[1] Mayumi Sasaki,[1] Yuichi Nishi,[1] Masato Okada,[3] and Nobuya Inagaki[1,4]

OBJECTIVE—Reactive oxygen species (ROS) is one of most important factors in impaired metabolism secretion coupling in pancreatic β-cells. We recently reported that elevated ROS production and impaired ATP production at high glucose in diabetic Goto-Kakizaki (GK) rat islets are effectively ameliorated by Src inhibition, suggesting that Src activity is upregulated. In the present study, we investigated whether the glucagon-like peptide-1 signal regulates Src activity and ameliorates endogenous ROS production and ATP production in GK islets using exendin-4.

RESEARCH DESIGN AND METHODS—Isolated islets from GK and control Wistar rats were used for immunoblotting analyses and measurements of ROS production and ATP content. Src activity was examined by immunoprecipitation of islet lysates followed by immunoblotting. ROS production was measured with a fluorescent probe using dispersed islet cells.

RESULTS—Exendin-4 significantly decreased phosphorylation of Src Tyr416, which indicates Src activation, in GK islets under 16.7 mmol/l glucose exposure. Glucose-induced ROS production (16.7 mmol/l) in GK islet cells was significantly decreased by coexposure of exendin-4 as well as PP2, a Src inhibitor. The Src kinase–negative mutant expression in GK islets significantly decreased ROS production induced by high glucose. Exendin-4, as well as PP2, significantly increased impaired ATP elevation by high glucose in GK islets. The decrease in ROS production by exendin-4 was not affected by H-89, a PKA inhibitor, and an Epac-specific cAMP analog (8CPT-2Me-cAMP) significantly decreased Src Tyr416 phosphorylation and ROS production.

CONCLUSIONS—Exendin-4 decreases endogenous ROS production and increases ATP production in diabetic GK rat islets through suppression of Src activation, dependently on Epac. ***Diabetes* 60:218–226, 2011**

From the [1]Department of Diabetes and Clinical Nutrition, Graduate School of Medicine, Kyoto, University, Kyoto, Japan; the [2]Japan Association for the Advancement of Medical Equipment, Tokyo, Japan, the [3]Department of Oncogene Research, Research Institute for Microbial Diseases, Osaka University, Osaka, Japan; and the [4]Core Research for Evolutional Science and Technology of Japan Science and Technology Cooperation, Kyoto, Japan.

Corresponding author: Shimpei Fujimoto, fujimoto@metab.kuhp.kyoto-u.ac.jp.

Received 6 January 2010 and accepted 12 October 2010. Published ahead of print at http://diabetes.diabetesjournals.org on 26 October 2010. DOI: 10.2337/db10-0021.

In pancreatic β-cells, glucose metabolism regulates exocytosis of insulin granules through metabolism secretion coupling, in which glucose-induced ATP production in mitochondria plays an essential role (1). Impairment of mitochondrial ATP production causes reduced glucose-induced insulin secretion.

Reactive oxygen species (ROS) is one of the most important factors that impair metabolism secretion coupling in β-cells. Exposure to exogenous hydrogen peroxide (H_2O_2), the most abundant ROS, reduces glucose-induced insulin secretion by impairing mitochondrial metabolism in β-cells (2,3). However, little is known of the role of endogenous ROS in impaired glucose-induced insulin secretion from β-cells. Some studies (4,5) have shown that endogenous ROS is produced in mitochondria by exposure to high glucose. In Zucker diabetic fatty rats, the superoxide content of islets at basal glucose levels is higher than that in Zucker lean control rats (4). Furthermore, we recently reported that high glucose–induced ROS production in islet cells is elevated in diabetic Goto-Kakizaki (GK) rats compared with control Wistar rats (6). Thus, endogenous ROS production is elevated in β-cells under diabetic pathophysiological conditions.

Although the mechanism of endogenous ROS production in β-cells in the diabetic state remains largely unknown, we have reported that Src (c-Src) plays an important role in the signal transduction that produces ROS (6). Src is a nonreceptor tyrosine kinase that is associated with the cell membrane and plays important roles in various signal transductions, and its activity is regulated by intramolecular interactions that depend on tyrosine phosphorylation (7,8). Phosphorylation of Tyr527 (Tyr529 in humans), which is located near the C terminus of Src, is brought about by COOH terminal Src kinase (Csk), a negative regulator of Src (9), and holds the kinase in the inactive form. Dephosphorylation of Tyr527 followed by disruption of the intramolecular interaction allows phosphorylation of Tyr416 (Tyr418 in humans) at the kinase domain, resulting in Src activation. In our previous report (6), PP2, a selective Src inhibitor, decreased high-glucose–induced ROS production in GK islet cells, in contrast to the lack of any effect of the agent in Wistar islet cells, suggesting that Src may be activated in the diabetic condition and cause elevation of ROS production in the presence of high glucose.

Glucagon-like peptide (GLP)-1 is one of the incretin peptides released from the intestine in response to nutrient ingestion that augments glucose-induced insulin secretion from β-cells (10,11). GLP-1 binding to the GLP-1 receptor, a member of the G protein–coupled receptor

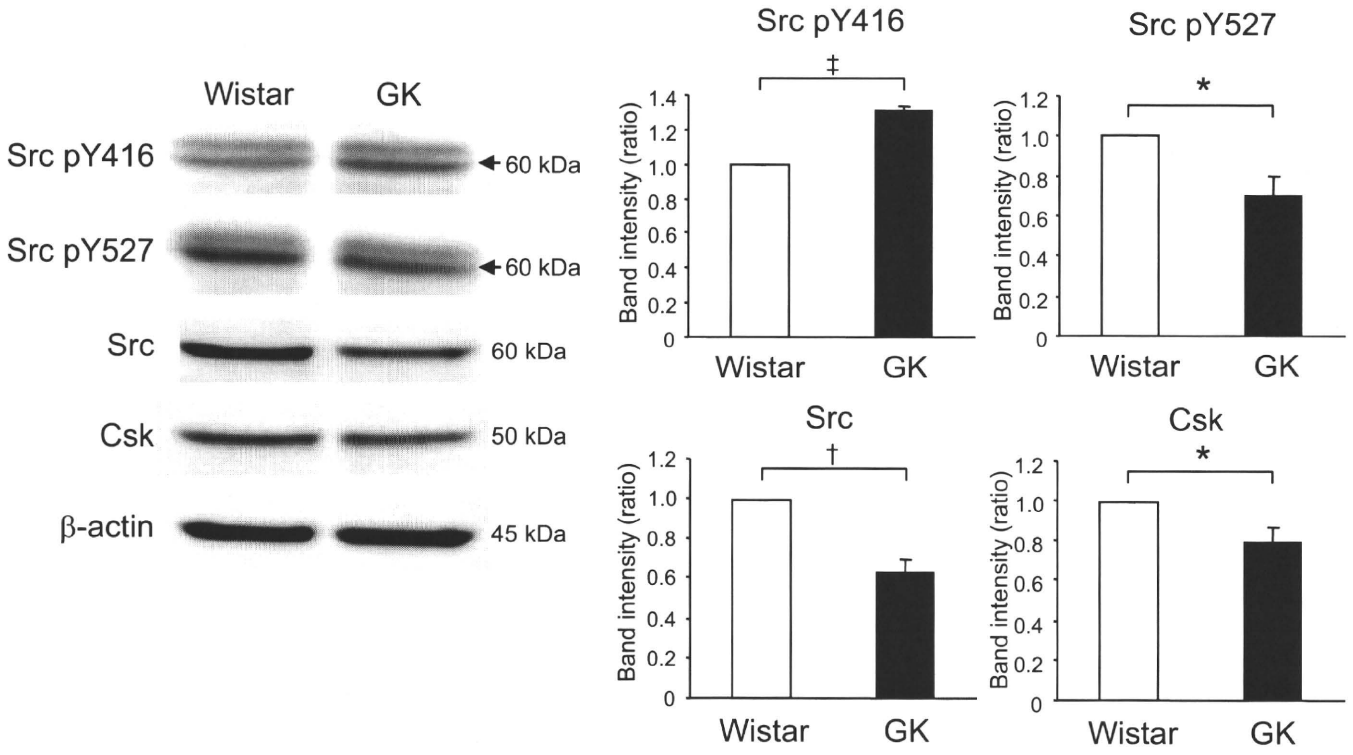

FIG. 1. Comparison of expression of Src between fresh Wistar and GK islets. Fresh islets were lysated and subjected to immunoblot analyses. Blots (50 μg of protein) were probed with anti–phospho-Src (Tyr^{416}), anti–phospho-Src (Tyr^{527}), anti-Src, or anti-Csk. The same blots were stripped and reprobed with anti–β-actin, respectively. Intensities of the bands were quantified with densitometric imager. The bar graphs are expressed relative to Wistar islet value corrected by β-actin level (means ± SE). *$P < 0.05$; †$P < 0.01$; ‡$P < 0.001$. Representative blot panels of three to five independent experiments are shown.

(GPCR) superfamily, induces activation of adenylyl cyclase and elevation of intracellular cAMP levels, which elicits protein kinase A (PKA)-dependent signal transduction. Recently, Epac (also known as cAMP-GEF [guanine nucleotide exchange factor]) has been shown to be a novel cAMP sensor in the PKA-independent pathway (12,13). In β-cells, one member of the Epac family, Epac2, has an important role in insulin secretion, especially in regulation of exocytosis of insulin granules (14,15). Previous studies have shown that GLP-1 also has beneficial long-term effects on diabetic β-cells, including induction of β-cell proliferation (16,17), enhanced resistance to apoptosis (17,18), and amelioration of endoplasmic reticulum stress (19). Furthermore, increased ROS in diabetic *db/db* mouse islets is decreased by treatment with an inhibitor of dipeptidyl peptidase IV that delays the degradation of GLP-1 (20).

In the present study, we investigated whether the GLP-1 signal directly ameliorates endogenous ROS production in diabetic GK islets using exendin-4, a GLP-1 receptor agonist. In particular, we focused on clarifying regulation of Src activity by GLP-1 signaling. We describe here both a novel effect and a mechanism of GLP-1 signaling that acutely decreases ROS production by high glucose through suppression of Src activation PKA independently and Epac dependently.

RESEARCH DESIGN AND METHODS

Male Wistar and GK rats were obtained from Shimizu (Kyoto, Japan). All experiments were carried out with rats that were aged ~7–8 weeks. Nonfasting blood glucose levels were ~160–240 mg/dl in the GK rats and ~70–120 mg/dl in the Wistar rats used in the experiments. The animals were maintained and used in accordance with the guidelines of the animal care committee of Kyoto University.

Islet preparation. Pancreatic islets were isolated from Wistar and GK rats by the collagenase digestion technique (6). Isolated islets were washed with Krebs Ringer bicarbonate buffer (KRBB) (in mmol/l: 129.4 NaCl, 5.2 KCl, 2.7 $CaCl_2$, 1.3 KH_2PO_4, 1.3 $MgSO_4$, and 24.8 $NaHCO_3$ [equilibrated with 5% CO_2/95% O_2, pH 7.4]) containing 2.8 mmol/l glucose and cultured for ~20 h in RPMI-1640 medium containing 5.5 mmol/l glucose and 10% FCS. Cultured islets were preincubated for 30 min at 37°C in KRBB supplemented with 0.2% BSA and 10 mmol/l HEPES (KRBB medium) containing 2.8 mmol/l glucose and incubated for the indicated times at 37°C in KRBB medium containing 16.7 mmol/l glucose with or without test materials.

Retroviral-mediated gene transfer. Production of retroviral vectors with pCX4 was performed as previously described (21). Src kinase–negative mutant (K295M) was subcloned into pCX4pur (22). Gene transfer experiments of islets were carried out by an in vivo gene transduction method (23). Briefly, after rats were anesthetized and subjected to laparotomy, the hepatic artery with the portal vein and the splenic artery were ligated. The upper side of the celiac artery that branches from the abdominal aorta was clamped, and 100 μl of retroviral vector suspension was injected into the lower side of the clamped point of the artery. The pancreatic islets were then isolated and cultured for 48 h before the experiment. Gene expression using green fluorescent protein–expressing vector was effective in the inside of the islets, as previously reported (23).

Immunoprecipitation and immunoblotting. Fresh or incubated islets were lysed in ice-cold lysis buffer (10 mmol/l Tris [pH 7.2], 100 mmol/l NaCl, 1 mmol/l EDTA, 1% Nonidet P-40, and 0.5% sodium deoxycholate) containing protease inhibitor cocktail (Complete; Roche, Mannheim, Germany), phosphatase inhibitor cocktail (Calbiochem, Darmstadt, Germany), and 5 mmol/l sodium pyrophosphate. For determination of Src activation, lysates were centrifuged at 560,000*g* for 10 min at 4°C, and the supernatant (~2 mg of protein content/2,500 islets) was mixed with 4 μg mouse monoclonal anti-Src antibody (clone GD11; Upstate, Billerica, MA) and 30 μl washed protein G Sepharose (GE Healthcare, Uppsala, Sweden) followed by gentle rotation for 4 h at 4°C. Immunoprecipitates or islet lysates (50 μg) were subjected to immunoblotting as previously described (23). Primary antibodies used were rabbit anti–phospho-Src (Tyr416) and anti–phospho-Src (Tyr527) from Biosource (Camarillo, CA); rabbit anti-Src, anti-Csk, anti-Epac2, extracellular signal–regulated kinase (ERK) 1/2, and mouse anti–phospho-ERK1/2 (Thr202/Tyr204) from Santa Cruz Biotechnology (Santa Cruz, CA); rabbit anti-Rap1 from Upstate; rabbit anti–phospho-Akt (Ser473) and anti-Akt from Cell

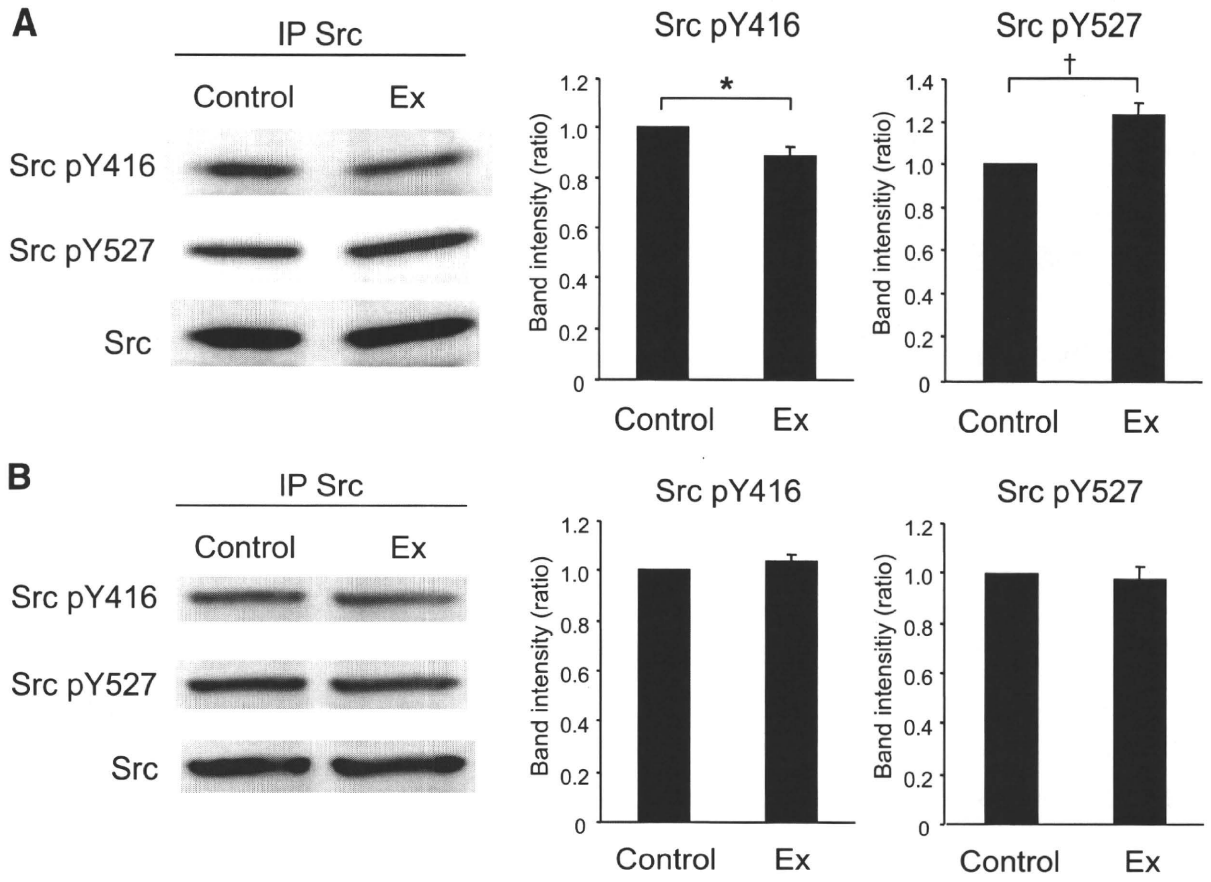

FIG. 2. Exendin-4 suppresses Src activity at high glucose in GK islets. Effects of exendin-4 on Src activity at high glucose in GK (*A*) and Wistar (*B*) islets. After preincubation in the presence of 2.8 mmol/l glucose for 30 min, islets were incubated in the presence of 16.7 mmol/l glucose with or without 100 nmol/l exendin-4 for 10 min. Islet lysates (~2 mg of protein) were immunoprecipitated with anti-Src antibody and subjected to immunoblot analyses. Blots were probed with anti–phospho-Src (Tyr^{416}), anti–phospho-Src (Tyr^{527}), or anti-Src by stripping and reprobing of the same blots. Intensities of the bands were quantified with densitometric imager. The bar graphs are expressed relative to control value corrected by Src level (means ± SE). *$P < 0.05$; †$P < 0.01$. Representative blot panels of four (*A*) or three (*B*) independent experiments are shown.

Signaling (Danvers, MA); and mouse anti–β-actin from Sigma (St. Louis, MO). Secondary antibodies used were horseradish peroxidase–conjugated anti-rabbit and mouse antibody (GE Healthcare). Band intensities were quantified with Multi Gauge software (Fujifilm, Tokyo, Japan).

Measurement of ROS production. ROS production in islet cells was measured by 2′,7′-dichlorofluorescein fluorescence (6). Briefly, cultured islets were dispersed using 0.05% trypsin/0.53 mmol/l EDTA (Invitrogen, Carlsbad, CA) and PBS. Dispersed islet cells were preincubated in KRBB medium containing 2.8 mmol/l glucose and 10 μmol/l 5-(and 6-) chloromethyl-2′,7′-dichlorodihydrofluorescein diacetate (CM-H_2DCFDA; Invitrogen) for 20 min at 37°C. After a 60-min incubation in 400 μl KRBB medium containing 16.7 mmol/l glucose with or without test materials, fluorescence was measured using a spectrofluorophotometer (RF-5300PC; Shimadzu, Kyoto, Japan), with excitation wavelength at 505 nm and emission wavelength at 540 nm. Fluorescence was corrected by subtracting parallel blanks and represented by fold increases of the value at time zero.

Measurement of ATP content. ATP content in islets was determined by luminometry as previously described (6). Briefly, after preincubation, groups of 10 islets were batch incubated for 30 min in KRBB medium containing 2.8 or 16.7 mmol/l glucose with or without test materials. Incubation was stopped immediately by addition of $HClO_4$ and sonication in ice-cold water for 10 min. They were then centrifuged, and a fraction of the supernatant was mixed with HEPES and Na_2CO_3. The ATP content in the supernatant of islet lysates was measured using ENLITEN luciferase/luciferin reagent (Promega, Madison, WI) with a luminometer (GloMax 20/20n; Promega).

Materials. Exendin-4 and forskolin were purchased from Sigma. PP2 was purchased from Tocris (Ellisville, MO). PP3, H-89, myristoylated PKA inhibitor amide14–22 (PKI), LY294002, wortmannin, PD98059, and AG1478 were purchased from Calbiochem. Dibutyryl cAMP was purchased from Daiichisankyo (Tokyo, Japan). 8-(4-chlorophenylthio)-2′-*O*-methyl-cAMP (8CPT-2Me-cAMP) was purchased from Biolog Life Science (Bremen, Germany).

Statistical analysis. Data are expressed as means ± SE. Statistical significance of difference was evaluated by the unpaired Student *t* test. $P < 0.05$ was considered significant.

RESULTS

Comparison of expression of Src between Wistar and GK islets. To examine whether the expression levels of Src in GK islets differ from those in Wistar islets, immunoblotting using fresh islets was performed. As shown in Fig. 1*A*, the level of Src pY416, which indicates activation of Src, in GK islets was significantly higher than that in Wistar islets. The levels of Src pY527, total Src, and Csk in GK islets were significantly lower than those in Wistar islets. The levels of other Src family kinases (SFKs) were similar in Wistar and GK islets, whereas the expression of Fgr was very low and that of Fyn was undetectable (supplementary Fig. 1 in the online appendix, available at http://diabetes.diabetesjournals.org/cgi/content/full/db10-0021/DC1). Results of immunoblotting using islets cultured for 20 h in the presence of 5.5 mmol/l glucose (supplementary Fig. 2) were similar to those shown in Fig. 1*A*.

Exendin-4 suppresses Src activity in GK islets. To investigate whether exendin-4 regulates Src activity, phosphorylation of Src was examined by immunoprecipitation and immunoblotting. As shown in Fig. 2*A*, Src pY416 was

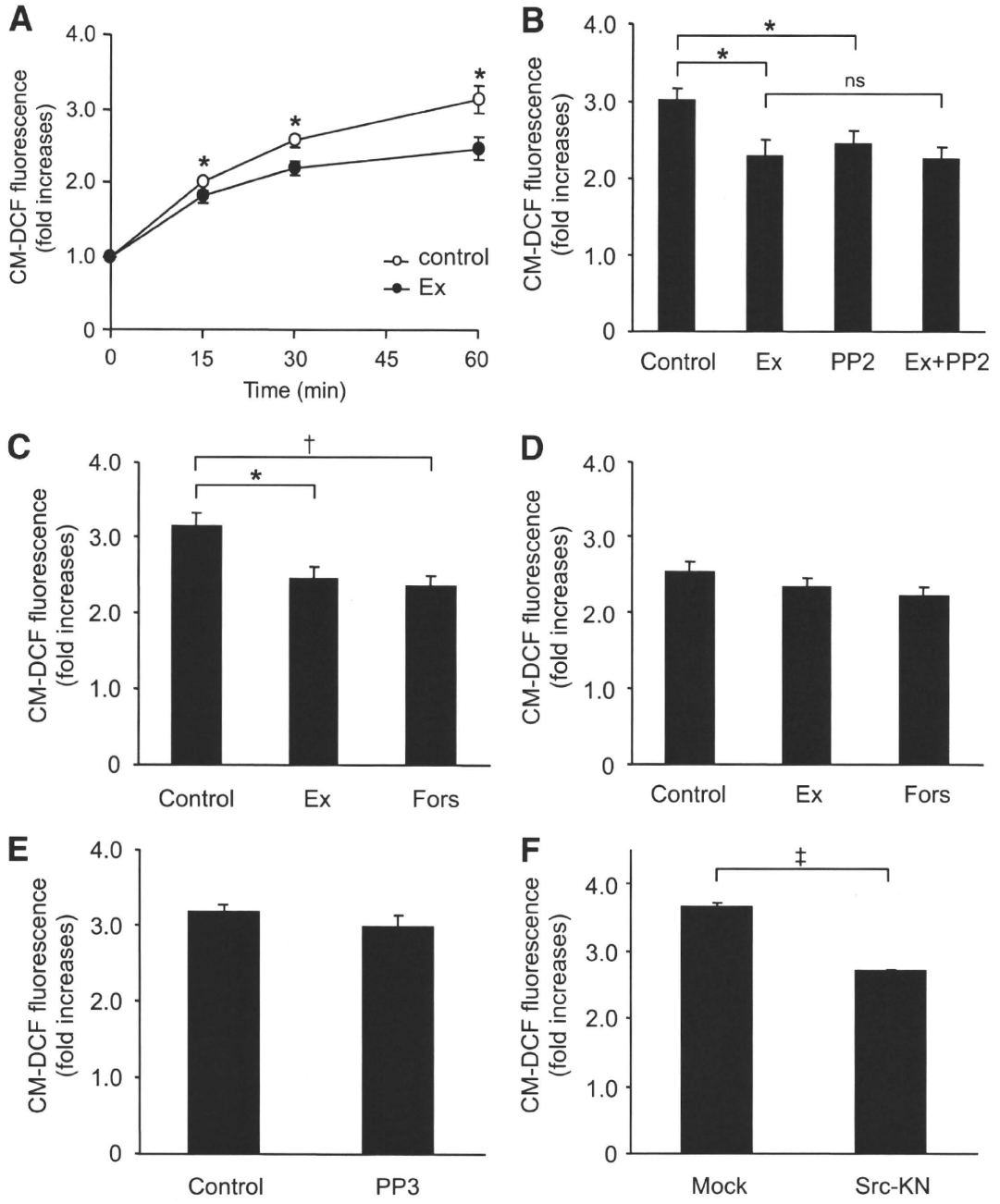

FIG. 3. Exendin-4 decreases ROS production at high glucose in GK islet cells. *A*: **Time course of high-glucose–induced ROS production with or without 100 nmol/l exendin-4 in GK islet cells. After preincubation in the presence of 2.8 mmol/l glucose and 10 μmol/l CM-H_2DCFDA for 20 min, dispersed islet cells were incubated in the presence of 16.7 mmol/l glucose with (●) or without (○) 100 nmol/l exedin-4 for 60 min. Fluorescence is represented as fold increases against the value at time zero. Data are expressed as means ± SE (n = 5–7). *P < 0.05 vs. control.** *B*: **Effects of exendin-4 and PP2 on high-glucose–induced ROS production at 60 min in GK islet cells. Data are expressed as means ± SE (n = 4–6). *P < 0.05.** *C*: **Effects of exendin-4 and forskolin on high-glucose–induced ROS production at 60 min in GK islet cells. Data are expressed as means ± SE (n = 5–6). *P < 0.05; †P < 0.01.** *D*: **Effects of exendin-4 and forskolin on high-glucose–induced ROS production at 60 min in Wistar islet cells. Data are expressed as means ± SE (n = 3–4).** *E*: **Effects of PP3 on high-glucose–induced ROS production at 60 min in GK islet cells. Data are expressed as means ± SE (n = 3).** *F*: **Effect of Src-KN on high-glucose–induced ROS production at 60 min in GK islet cells. Retroviral (empty vector and Src-KN vector)-mediated gene transfer to islets was carried out by in vivo gene transduction method, as described in RESEARCH DESIGN AND METHODS. Data are expressed as means ± SE (n = 3). ‡P < 0.001.**

significantly decreased by 100 nmol/l exendin-4 in the presence of 16.7 mmol/l glucose in GK islets. Exendin-4 also significantly increased Src pY527 in GK islets in the same condition. On the other hand, exendin-4 did not affect Src pY416 or pY527 at high glucose in Wistar islets (Fig. 2*B*). Both Src pY416 and pY527 were not altered by change in glucose concentration in GK or Wistar islets (supplementary Fig. 3).

Exendin-4 decreases ROS production in GK islet cells. We then investigated whether exendin-4 ameliorates endogenous ROS production at high glucose in GK islet cells. A total of 16.7 mmol/l glucose exposure induced ROS production in GK islet cells (Fig. 3*A*). Coexposure of exendin-4 significantly decreased ROS production in the presence of 16.7 mmol/l glucose at 15, 30, and 60 min. A total of 10 μmol/l PP2, a Src inhibitor, significantly de-

creased high-glucose–induced ROS production (Fig. 3*B*), but PP3, the inactive PP2 analog, did not affect it (Fig. 3*E*). Exendin-4 did not further decrease ROS production in the presence of PP2 (Fig. 3*B*), suggesting that the effect of exendin-4 is via the Src signal. The decrease in high-glucose–induced ROS production also was observed in the presence of 10 μmol/l forskolin, an adenylyl cyclase activator (Fig. 3*C*). High-glucose–induced ROS production in Wistar islet cells was lower than that in GK islet cells and was not changed by addition of exendin-4 or forskolin (Fig. 3*D*). To confirm that Src is actually involved in ROS production, we measured ROS production in GK islets expressing a kinase-negative form of Src (Src-KN) by retroviral vector. ROS production in Src-KN–expressing islets was significantly lower than that in control (Fig. 3*F*), demonstrating that Src regulates ROS production in GK islets.

Exendin-4 increases ATP content in GK islets. In Wistar islets, 16.7 mmol/l glucose-exposure significantly increased ATP content compared with that in the presence of 2.8 mmol/l glucose, as shown in Fig. 4*B*. Exendin-4, PP2, or exendin-4 plus PP2 did not affect the ATP content in the presence of 16.7 mmol/l glucose in Wistar islets. The ATP content in GK islets exposed to 16.7 mmol/l glucose was not increased compared with that in the presence of 2.8 mmol/l glucose (Fig. 4*A*). Exendin-4 as well as PP2 significantly increased the ATP content in the presence of 16.7 mmol/l glucose. Further increase of ATP content by combined exendin-4 and PP2 was not observed.

The effects of exendin-4 are dependent on Epac. We then investigated whether the decrease in ROS production by exendin-4 is dependent on PKA. As shown in Fig. 5*A*, decreased ROS production by exendin-4 or forskolin was not affected by 10 μmol/l H-89 or PKI, a PKA inhibitor, indicating that the effect is PKA independent. Not only dibutyryl cAMP, a general cAMP analog, but also 8CPT-2Me-cAMP, an Epac-specific cAMP analog, decreased ROS production (Fig. 5*C*). Epac possesses guanine nucleotide exchange factor activity toward Rap1, a member of the Ras superfamily of small GTPases. Epac2 and Rap1 proteins were expressed similarly in both Wistar and GK islets (Fig. 5*B*). To determine involvement of Epac in Src activation, Src phosphorylation was examined. Src pY416 was significantly decreased by 8CPT-2Me-cAMP (Fig. 5*D*).

A downstream pathway of Src is PI3K/Akt signaling. Src signalings toward downstream proteins are complex, but one of the typical pathways is phosphatidylinositol 3 kinase (PI3K)/Akt signaling (8). We therefore examined the involvement of PI3K/Akt signaling on ROS production. A total of 50 μmol/l LY294002 and 0.5 μmol/l wortmannin, both of which are PI3K inhibitors, significantly decreased ROS production in GK islets (Fig. 6*A*). Exendin-4 and PP2 both significantly decreased phosphorylation of Akt in GK islets (Fig. 6*B*) but not in Wistar islets (Fig. 6*C*). Considering these findings together, PI3K/Akt signaling that produces ROS is located downstream of Src activation. We also examined the involvement of mitogen-activated protein kinase signaling, another downstream pathway of Src. A total of 50 μmol/l PD98059, a MAPK-ERK kinase inhibitor, did not affect ROS production in GK islets (Fig. 6*D*), and neither exendin-4 nor PP2 affected phosphorylation of ERK (Fig. 6*E*). Several GPCR agonists have been shown to induce transactivation of epidermal growth factor receptor (EGFR) (24,25) by a mechanism involving Src (25–27) and frequently subsequent PI3K/Akt signaling (25,28). Therefore, involvement of EGFR transactivation on regulation of ROS production was examined. A total of 0.5 μmol/l AG1478, an EGFR kinase inhibitor, significantly decreased ROS production (Fig. 6*F*).

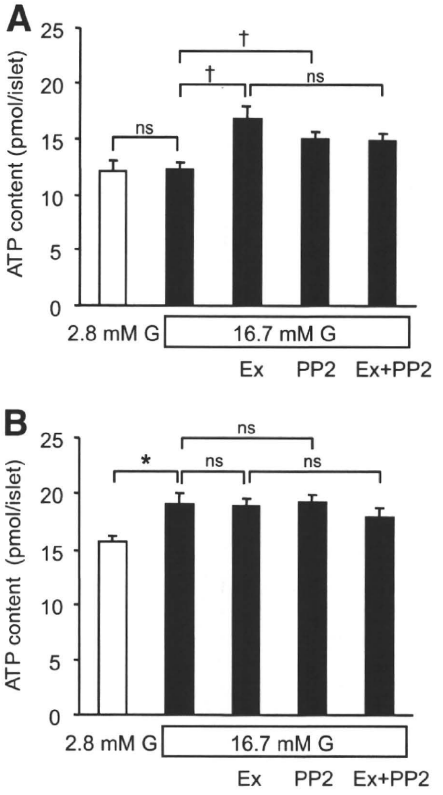

FIG. 4. Exendin-4 increases ATP content at high glucose in GK islets. Effects of exendin-4 and PP2 on ATP content in the presence of high glucose for 30 min in GK (*A*) and Wistar (*B*) islets. After preincubation in the presence of 2.8 mmol/l glucose for 30 min, islets were incubated in the presence of 2.8 or 16.7 mmol/l glucose with or without 100 nmol/l exendin-4, 10 μmol/l PP2, or both for 30 min. Data are expressed as means ± SE (n = 7–8). *P < 0.05; †P < 0.01.

DISCUSSION

We previously reported that endogenous ROS production by high glucose in diabetic GK islets is elevated compared with that in control Wistar islets and is effectively ameliorated by Src inhibition, suggesting that Src may be activated in GK islets (6). In the present study, we first investigated whether Src activity is altered in GK islets. Immunoblotting analysis revealed that the level of Src pY416, which indicates the level of Src activation, is higher in GK islets than that in Wistar islets, despite lower levels of total Src, Src pY527, and Csk. The lower level of total Src seems to be a consequence of Src activation. Targeted degradation of active forms of Src is brought about by ubiquitination (29). The protooncogene c-Cbl, recently found to be an E3 ubiquitin ligase, mediates ubiquitination of activated Src (30). These reports suggest that increased degradation of activated Src may result in a lower level of total Src in GK islets. In addition, a lower level of Csk might cause a lower activity of the kinase in GK islets. However, Src activity is not directly regulated through phosphorylation of Tyr527 by Csk (8), and a subtle decrease in Csk activity is not believed to contribute to regulation of Src activity because of the excess amount of expression of Csk. This is supported by the findings that heterozygous disruption of ubiquitously expressed Csk

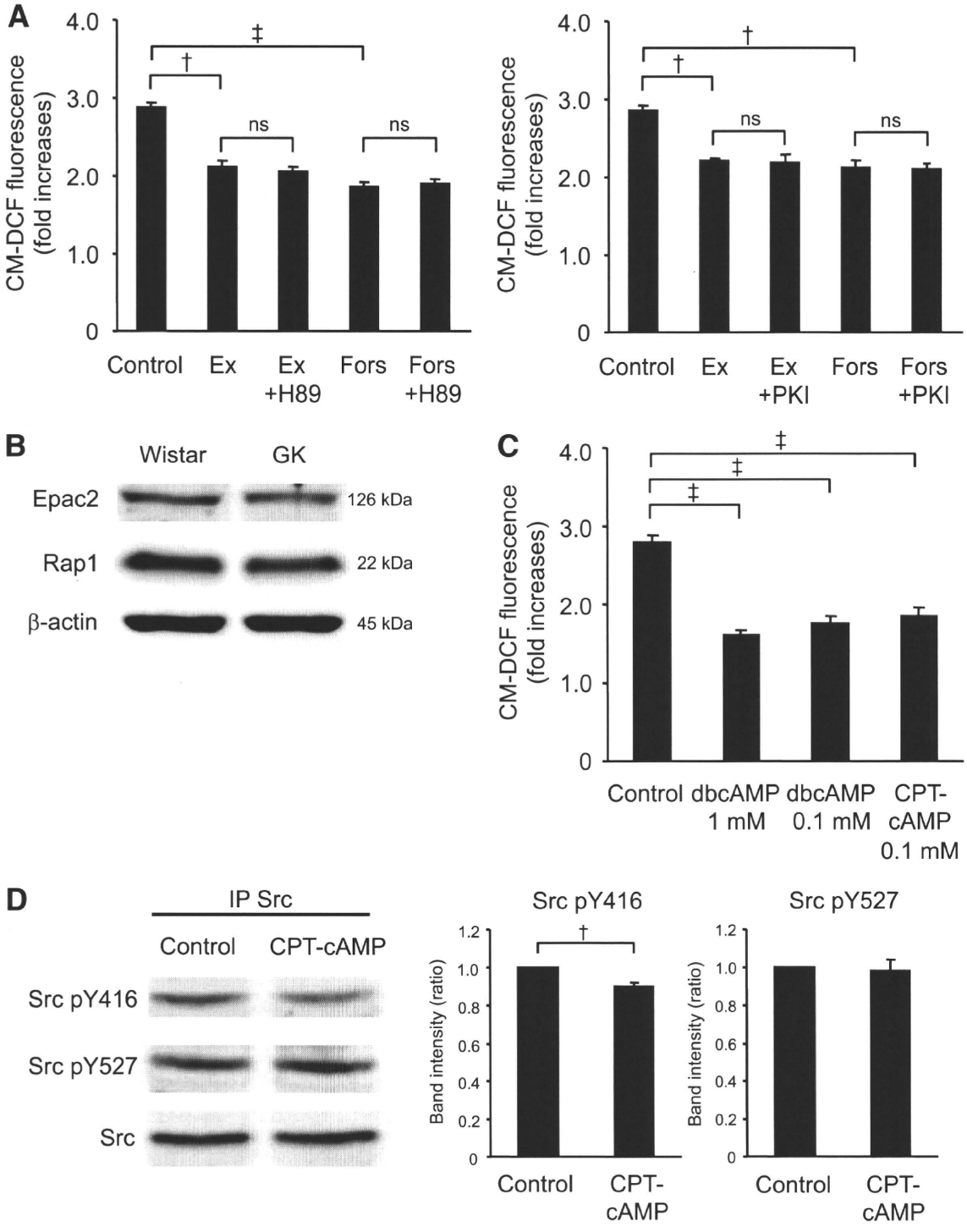

FIG. 5. The effects of exendin-4 are dependent not on PKA but on Epac. *A*: Effects of H-89 or PKI on the decrease in high-glucose–induced ROS production by exendin-4 or forskolin at 60 min in GK islet cells. After preincubation in the presence of 2.8 mmol/l glucose and 10 μmol/l CM-H_2DCFDA for 20 min, dispersed islet cells were incubated in the presence of 16.7 mmol/l glucose with or without 100 nmol/l exendin-4 or 10 μmol/l forskolin with or without 10 μmol/l H-89 or 10 μmol/l PKI for 60 min. Fluorescence is represented as fold increases against the value at time zero. Data are expressed as means ± SE (n = 3). †P < 0.01; ‡P < 0.001. *B*: Expression of Epac2 and Rap1 in Wistar and GK islets. Fresh islets were lysated and subjected to immunoblot analyses. Blots (50 μg of protein) were probed with anti-Epac2 or anti-Rap1. The same blots were stripped and reprobed with anti–β-actin, respectively. Representative blot panels of three independent experiments are shown. *C*: Effects of cAMP analogs on high-glucose–induced ROS production at 60 min in GK islet cells. Data are expressed as means ± SE (n = 3–4). ‡P < 0.001. *D*: Epac-specific cAMP analog suppresses Src activity at high glucose in GK islets. After preincubation in the presence of 2.8 mmol/l glucose for 30 min, islets were incubated in the presence of 16.7 mmol/l glucose with or without 0.1 mmol/l 8CPT-2Me-cAMP for 8 min. Islet lysates (~2 mg of protein) were immunoprecipitated with anti-Src antibody and subjected to immunoblot analyses. Blots were probed with anti–phospho-Src (Tyr^{416}), anti–phospho-Src (Tyr^{527}), or anti-Src by stripping and reprobing of the same blots. Intensities of the bands were quantified with densitometric imager. The bar graphs are expressed relative to control value corrected by Src level (means ± SE). †P < 0.01. Representative blot panels of four independent experiments are shown.

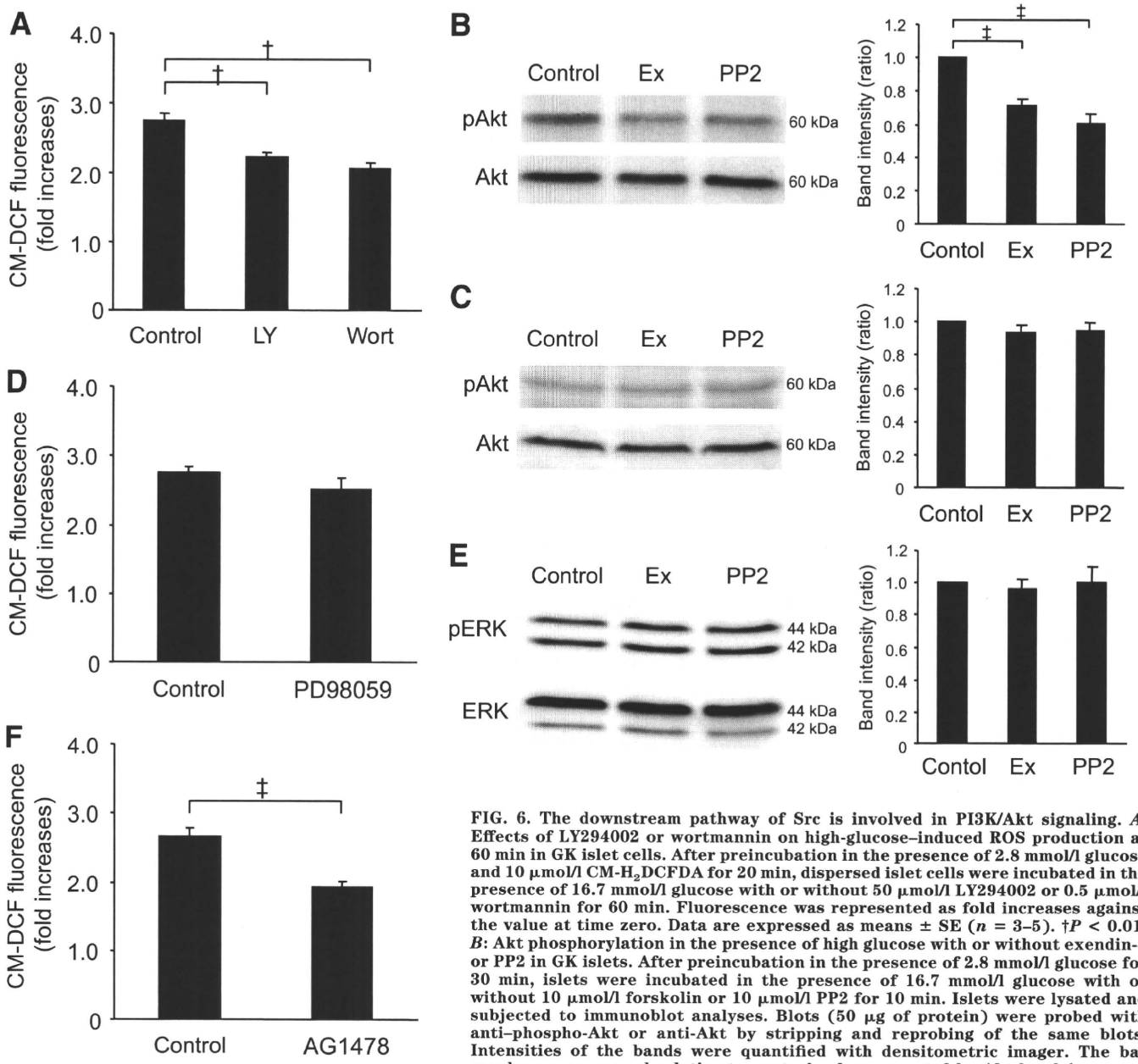

FIG. 6. The downstream pathway of Src is involved in PI3K/Akt signaling. *A*: Effects of LY294002 or wortmannin on high-glucose–induced ROS production at 60 min in GK islet cells. After preincubation in the presence of 2.8 mmol/l glucose and 10 μmol/l CM-H_2DCFDA for 20 min, dispersed islet cells were incubated in the presence of 16.7 mmol/l glucose with or without 50 μmol/l LY294002 or 0.5 μmol/l wortmannin for 60 min. Fluorescence was represented as fold increases against the value at time zero. Data are expressed as means ± SE (n = 3–5). †P < 0.01. *B*: Akt phosphorylation in the presence of high glucose with or without exendin-4 or PP2 in GK islets. After preincubation in the presence of 2.8 mmol/l glucose for 30 min, islets were incubated in the presence of 16.7 mmol/l glucose with or without 10 μmol/l forskolin or 10 μmol/l PP2 for 10 min. Islets were lysated and subjected to immunoblot analyses. Blots (50 μg of protein) were probed with anti–phospho-Akt or anti-Akt by stripping and reprobing of the same blots. Intensities of the bands were quantified with densitometric imager. The bar graphs are expressed relative to control value corrected by Akt level (means ± SE). ‡P < 0.001. Representative blot panels of five independent experiments are shown. *C*: Akt phosphorylation in the presence of high glucose with or without exendin-4 or PP2 in Wistar islets. Representative blot panels of three independent experiments are shown. *D*: Effects of PD98059 on high-glucose–induced ROS production at 60 min in GK islet cells. Data are expressed as means ± SE (n = 4). *E*: ERK phosphorylation in the presence of high glucose with or without exendin-4 or PP2 in GK islets. Blots (50 μg of protein) were probed with anti–phospho-ERK or anti-ERK by stripping and reprobing of the same blots. The bar graphs are expressed relative to control value corrected by ERK level (means ± SE). Representative blot panels of three independent experiments are shown. *F*: Effects of AG1478 on high-glucose–induced ROS production at 60 min in GK islet cells. Data are expressed as means ± SE (n = 5). ‡P < 0.001.

does not affect the phenotype in mice, contrary to neural tube defects and embryonic lethality in homozygous deficient mice (31). Moreover, the localization of Csk in the cytosol before recruitment to the membrane for Src regulation dose not differ in Wistar and GK islets (supplementary Fig. 4). Thus, the lower expression level of Csk found in our results is not likely to play a role in the Src activation in GK islets. Activation of Src as well as elevated endogenous ROS production at high glucose in GK islets was clearly suppressed by exendin-4, which did not affect Src phosphorylation or ROS production in Wistar islets. Thus, the GLP-1 signal might well suppress activation of Src and excessive ROS production under diabetic conditions in addition to other beneficial long-term effects on β-cells.

GLP-1 induces elevation of intracellular cAMP levels and subsequent activation of PKA after binding to the GLP-1 receptor. In the present study, the effect of GLP-1 signaling, which suppresses Src activation and ROS production, was found to be independent of PKA. Epac is a PKA-independent cAMP sensor; Epac2 is expressed mainly in neuroendocrine cells including pancreatic β-cells. Epac2 regulates exocytosis of insulin granules in β-cells by mobilizing intracellular Ca^{2+} and interacting granule-associated proteins (14,15). Although the relationship between Epac and Src is not well known, a recent

report (32) has shown that cAMP protects against hepatocyte apoptosis Epac dependently through Src and PI3K/Akt activation. Further evaluation of the role of cAMP in regulation of Src and PI3K/Akt signaling is required.

In the present study, we have shown that one of these Src signals, the PI3K/Akt signal, regulates ROS production. Furthermore, GLP-1 induces β-cell proliferation through PI3K signaling via Src and EGFR transactivation (33). Our finding that the EGFR kinase inhibitor decreases ROS production suggests that EGFR transactivation may be involved in the ROS-reducing effect of exendin-4 via Src. Under normal conditions, GPCR stimulation generally activates Src toward EGFR transactivation, frequently followed by PI3K activation (25). The present study reveals that Src and PI3K activities are upregulated in islets under diabetic conditions, which are suppressed by the GLP-1 signal. Many studies in oncology have shown that several growth factors including EGF and platelet-derived growth factor induce ROS through PI3K activation (34–36). Thus, EGFR transactivation/PI3K signaling should be activated under pathophysiologically disordered conditions. In the various states between normal and diabetic conditions, the ameliorative effects of the GLP-1 signal may differ (37). Further elucidation of these signals in the pathophysiology of diabetes should be helpful in future development of therapeutic strategies.

Previous studies have shown that the antioxidant capacity in β-cells is very low because of weak expression of antioxidant enzymes in pancreatic islets compared with that in various other tissues (38). The superoxide anion is converted by superoxide dismutase (SOD) into hydrogen peroxide that is eventually removed by glutathione peroxidase (Gpx). The expression level of MnSOD, which is localized in mitochondria, was significantly lower in GK islets than in Wistar islets, and that of of Gpx was similar in Wistar and GK islets (supplementaty Fig. 5*A*). However, an enzymatic assay revealed that MnSOD activity in GK islets was similar to that in Wistar islets and that it was not affected by exendin-4 or PP2 (supplementary Fig. 5*B* and *C*). These results indicate that regulation of MnSOD activity does not play a role in the suppressive effects of ROS production by exendin-4.

One of the important sites of ROS generation in β-cells is the mitochondrial electron transport chain, in which ROS generation increases according to the hyperpolarization of mitochondrial inner membrane derived from accelerated glucose metabolism (39). However, in pathophysiological conditions, NADPH oxidase may play an important role in ROS generation in β-cells. Chronic exposure to proinflammatory cytokines and abundant nutrients including glucose and palmitate augments the expression of a phagocyte-like NADPH oxidase in β-cells (40). Moreover, the expression of NADPH oxidase is increased in islets of diabetic Otsuka Long Evans Tokushima Fatty rats (41). Because Src is involved in regulation of NADPH oxidase activity (42), further examination to elucidate the site of ROS generation related to Src activation in β-cells is needed. On the other hand, previous reports have shown that ROS itself regulates Src activity (43,44) in addition to Src activity regulation of ROS production (45). To clarify this mutual causal relationship between Src and ROS, we examined ROS production in GK islets expressing Src-KN, which was found to cause a distinct decrease in high-glucose–induced ROS production. This finding demonstrates that Src activity regulates ROS production and does not contradict the possibility of a feedback regulation mechanism of ROS on Src activity (45).

The high-glucose–induced increase in ATP production is impaired in GK rats (6,46) as well as in patients with type 2 diabetes (47). In addition, islets in GK rats and human type 2 diabetes are oxidatively stressed (48–50). In the present study, exendin-4 was able to recover this impaired increase in ATP production by high glucose in GK islets as well as to decrease excessive ROS production. Thus, GLP-1 signaling may improve β-cell function in the diabetic state not only because it enhances Ca^{2+} efficacy of the exocytotic system of insulin granules but also because it improves impaired metabolism-secretion coupling. GLP-1 receptor agonists are widely used in treatment of type 2 diabetes for their ability to improve glucose intolerance. Their clinical beneficial effect seems to be provided not only by their insulinotropic action but also by their reduction of β-cell apoptosis and induction of β-cell proliferation (16–18). Further elucidation of endogenous ROS regulation by GLP-1 may help to clarify the mechanism of the various beneficial effects of these agents.

ACKNOWLEDGMENTS

This work was supported by a research grant on Nanotechnical Medicine from the Ministry of Health, Labor, and Welfare of Japan; by scientific research grants from the Ministry of Education, Culture, Sports, Science, and Technology of Japan; and also by the Kyoto University Global Center of Excellence Program Center for Frontier Medicine.

No potential conflicts of interest relevant to this article were reported.

E.M. researched data, contributed to the discussion, wrote the manuscript, and reviewed/edited the manuscript. S.F. contributed to the discussion, wrote the manuscript, and reviewed/edited the manuscript. H.S., C.O., R.K., Y.S., M.S., and Y.N. researched data. M.O. contributed to the discussion and reviewed/edited the manuscript. N.I. contributed to the discussion and reviewed/edited the manuscript.

Parts of this study were presented in abstract form at the 70th Scientific Sessions of the American Diabetes Association, Orlando, Florida, 25–29 June 2010.

We acknowledge the editorial assistance of Dalmen Mayer. We thank C. Kotake for excellent technical assistance.

REFERENCES

1. Maechler P, Wollheim CB. Mitochondrial function in normal and diabetic beta-cells. Nature 2001;414:807–812
2. Krippeit-Drews P, Kramer C, Welker S, Lang F, Ammon HP, Drews G. Interference of H2O2 with stimulus-secretion coupling in mouse pancreatic beta-cells. J Physiol 1999;514(Pt 2):471–481
3. Maechler P, Jornot L, Wollheim CB. Hydrogen peroxide alters mitochondrial activation and insulin secretion in pancreatic beta cells. J Biol Chem 1999;274:27905–27913
4. Bindokas VP, Kuznetsov A, Sreenan S, Polonsky KS, Roe MW, Philipson LH. Visualizing superoxide production in normal and diabetic rat islets of Langerhans. J Biol Chem 2003;278:9796–9801
5. Sakai K, Matsumoto K, Nishikawa T, Suefuji M, Nakamaru K, Hirashima Y, Kawashima J, Shirotani T, Ichinose K, Brownlee M, Araki E. Mitochondrial reactive oxygen species reduce insulin secretion by pancreatic beta-cells. Biochem Biophys Res Commun 2003;300:216–222
6. Kominato R, Fujimoto S, Mukai E, Nakamura Y, Nabe K, Shimodahira M, Nishi Y, Funakoshi S, Seino Y, Inagaki N. Src activation generates reactive oxygen species and impairs metabolism-secretion coupling in diabetic Goto-Kakizaki and ouabain-treated rat pancreatic islets. Diabetologia 2008;51:1226–1235
7. Xu W, Harrison SC, Eck MJ. Three-dimensional structure of the tyrosine kinase c-Src. Nature 1997;385:595–602

8. Martin GS. The hunting of the Src. Nat Rev Mol Cell Biol 2001;2:467–475
9. Nada S, Okada M, MacAuley A, Cooper JA, Nakagawa H. Cloning of a complementary DNA for a protein-tyrosine kinase that specifically phosphorylates a negative regulatory site of p60c-src. Nature 1991;351: 69–72
10. Baggio LL, Drucker DJ. Biology of incretins: GLP-1 and GIP. Gastroenterology 2007;132:2131–2157
11. Holst JJ. The physiology of glucagon-like peptide 1. Physiol Rev 2007;87: 1409–1439
12. Seino S, Shibasaki T. PKA-dependent and PKA-independent pathways for cAMP-regulated exocytosis. Physiol Rev 2005;85:1303–1342
13. Roscioni SS, Elzinga CR, Schmidt M. Epac: effectors and biological functions. Naunyn Schmiedebergs Arch Pharmacol 2008;377:345–357
14. Ozaki N, Shibasaki T, Kashima Y, Miki T, Takahashi K, Ueno H, Sunaga Y, Yano H, Matsuura Y, Iwanaga T, Takai Y, Seino S. cAMP-GEFII is a direct target of cAMP in regulated exocytosis. Nat Cell Biol 2000;2:805–811
15. Kang G, Joseph JW, Chepurny OG, Monaco M, Wheeler MB, Bos JL, Schwede F, Genieser HG, Holz GG. Epac-selective cAMP analog 8-pCPT-2′-O-Me-cAMP as a stimulus for Ca2+-induced Ca2+ release and exocytosis in pancreatic beta-cells. J Biol Chem 2003;278:8279–8285
16. Xu G, Stoffers DA, Habener JF, Bonner-Weir S. Exendin-4 stimulates both β-cell replication and neogenesis, resulting in increased β-cell mass and improved glucose tolerance in diabetic rats. Diabetes 1999; 48:2270–2276
17. Farilla L, Hui H, Bertolotto C, Kang E, Bulotta A, Di Mario U, Perfetti R. Glucagon-like peptide-1 promotes islet cell growth and inhibits apoptosis in Zucker diabetic rats. Endocrinology 2002;143:4397–4408
18. Li Y, Hansotia T, Yusta B, Ris F, Halban PA, Drucker DJ. Glucagon-like peptide-1 receptor signaling modulates beta cell apoptosis. J Biol Chem 2003;278:471–478
19. Tsunekawa S, Yamamoto N, Tsukamoto K, Itoh Y, Kaneko Y, Kimura T, Ariyoshi Y, Miura Y, Oiso Y, Niki I. Protection of pancreatic beta-cells by exendin-4 may involve the reduction of endoplasmic reticulum stress; in vivo and in vitro studies. J Endocrinol 2007;193:65–74
20. Cheng Q, Law PK, de Gasparo M, Leung PS. Combination of the dipeptidyl peptidase IV inhibitor LAF237 [(S)-1-[(3-hydroxy-1-adamantyl)ammo]acetyl-2-cyanopyrrolidine] with the angiotensin II type 1 receptor antagonist valsartan [N-(1-oxopentyl)-N-[[2′-(1H-tetrazol-5-yl)-[1,1′-biphenyl]-4-yl]methyl]-L-valine] enhances pancreatic islet morphology and function in a mouse model of type 2 diabetes. J Pharmacol Exp Ther 2008;327:683–691
21. Akagi T, Sasai K, Hanafusa H. Refractory nature of normal human diploid fibroblasts with respect to oncogene-mediated transformation. Proc Natl Acad Sci U S A 2003;100:13567–13572
22. Florio M, Wilson LK, Trager JB, Thorner J, Martin GS. Aberrant protein phosphorylation at tyrosine is responsible for the growth-inhibitory action of pp60v-src expressed in the yeast Saccharomyces cerevisiae. Mol Biol Cell 1994;5:283–296
23. Mukai E, Fujimoto S, Sakurai F, Kawabata K, Yamashita M, Inagaki N, Mizuguchi H. Efficient gene transfer into murine pancreatic islets using adenovirus vectors. J Control Release 2007;119:136–141
24. Daub H, Weiss FU, Wallasch C, Ullrich A. Role of transactivation of the EGF receptor in signalling by G-protein-coupled receptors. Nature 1996; 379:557–560
25. Rozengurt E. Mitogenic signaling pathways induced by G protein-coupled receptors. J Cell Physiol 2007;213:589–602
26. Eguchi S, Iwasaki H, Inagami T, Numaguchi K, Yamakawa T, Motley ED, Owada KM, Marumo F, Hirata Y. Involvement of PYK2 in angiotensin II signaling of vascular smooth muscle cells. Hypertension 1999;33:201–206
27. Gao Y, Tang S, Zhou S, Ware JA. The thromboxane A2 receptor activates mitogen-activated protein kinase via protein kinase C-dependent Gi coupling and Src-dependent phosphorylation of the epidermal growth factor receptor. J Pharmacol Exp Ther 2001;296:426–433
28. Chiu T, Santiskulvong C, Rozengurt E. EGF receptor transactivation mediates ANG II-stimulated mitogenesis in intestinal epithelial cells through the PI3-kinase/Akt/mTOR/p70S6K1 signaling pathway. Am J Physiol Gastrointest Liver Physiol 2005;288:G182–G194
29. Harris KF, Shoji I, Cooper EM, Kumar S, Oda H, Howley PM. Ubiquitin-mediated degradation of active Src tyrosine kinase. Proc Natl Acad Sci U S A 1999;96:13738–13743
30. Yokouchi M, Kondo T, Sanjay A, Houghton A, Yoshimura A, Komiya S, Zhang H, Baron R. Src-catalyzed phosphorylation of c-Cbl leads to the interdependent ubiquitination of both proteins. J Biol Chem 2001;276: 35185–35193
31. Nada S, Yagi T, Takeda H, Tokunaga T, Nakagawa H, Ikawa Y, Okada M, Aizawa S. Constitutive activation of Src family kinases in mouse embryos that lack Csk. Cell 1993;73:1125–1135
32. Gates A, Hohenester S, Anwer MS, Webster CR. cAMP-GEF cytoprotection by Src tyrosine kinase activation of phosphoinositide-3-kinase p110 beta/alpha in rat hepatocytes. Am J Physiol Gastrointest Liver Physiol 2009;296: G764–G774
33. Buteau J, Foisy S, Joly E, Prentki M. Glucagon-like peptide 1 induces pancreatic β-cell proliferation via transactivation of the epidermal growth factor receptor. Diabetes 2003;52:124–132
34. Zhu QS, Xia L, Mills GB, Lowell CA, Touw IP, Corey SJ. G-CSF induced reactive oxygen species involves Lyn-PI3-kinase-Akt and contributes to myeloid cell growth. Blood 2006;107:1847–1856
35. Baumer AT, Ten Freyhaus H, Sauer H, Wartenberg M, Kappert K, Schnabel P, Konkol C, Hescheler J, Vantler M, Rosenkranz S. Phosphatidylinositol 3-kinase-dependent membrane recruitment of Rac-1 and p47phox is critical for alpha-platelet-derived growth factor receptor-induced production of reactive oxygen species. J Biol Chem 2008;283:7864–7876
36. Binker MG, Binker-Cosen AA, Richards D, Oliver B, Cosen-Binker LI. EGF promotes invasion by PANC-1 cells through Rac1/ROS-dependent secretion and activation of MMP-2. Biochem Biophys Res Commun 2009;379: 445–450
37. Peyot ML, Gray JP, Lamontagne J, Smith PJ, Holz GG, Madiraju SR, Prentki M, Heart E. Glucagon-like peptide-1 induced signaling and insulin secretion do not drive fuel and energy metabolism in primary rodent pancreatic beta-cells. PLoS One 2009;4:e6221
38. Tiedge M, Lortz S, Drinkgern J, Lenzen S. Relation between antioxidant enzyme gene expression and antioxidative defense status of insulin-producing cells. Diabetes 1997;46:1733–1742
39. Newsholme P, Haber EP, Hirabara SM, Rebelato EL, Procopio J, Morgan D, Oliveira-Emilio HC, Carpinelli AR, Curi R. Diabetes associated cell stress and dysfunction: role of mitochondrial and non-mitochondrial ROS production and activity. J Physiol 2007;583:9–24
40. Morgan D, Oliveira-Emilio HR, Keane D, Hirata AE, Santos da Rocha M, Bordin S, Curi R, Newsholme P, Carpinelli AR. Glucose, palmitate and pro-inflammatory cytokines modulate production and activity of a phagocyte-like NADPH oxidase in rat pancreatic islets and a clonal beta cell line. Diabetologia 2007;50:359–369
41. Nakayama M, Inoguchi T, Sonta T, Maeda Y, Sasaki S, Sawada F, Tsubouchi H, Sonoda N, Kobayashi K, Sumimoto H, Nawata H. Increased expression of NAD(P)H oxidase in islets of animal models of Type 2 diabetes and its improvement by an AT1 receptor antagonist. Biochem Biophys Res Commun 2005;332:927–933
42. Chowdhury AK, Watkins T, Parinandi NL, Saatian B, Kleinberg ME, Usatyuk PV, Natarajan V. Src-mediated tyrosine phosphorylation of p47phox in hyperoxia-induced activation of NADPH oxidase and generation of reactive oxygen species in lung endothelial cells. J Biol Chem 2005;280:20700–20711
43. Giannoni E, Buricchi F, Raugei G, Ramponi G, Chiarugi P. Intracellular reactive oxygen species activate Src tyrosine kinase during cell adhesion and anchorage-dependent cell growth. Mol Cell Biol 2005;25:6391–6403
44. Zhang J, Xing D, Gao X. Low-power laser irradiation activates Src tyrosine kinase through reactive oxygen species-mediated signaling pathway. J Cell Physiol 2008;217:518–528
45. Xie Z, Cai T. Na+-K+-ATPase-mediated signal transduction: from protein interaction to cellular function. Mol Interv 2003;3:157–168
46. Hughes SJ, Faehling M, Thorneley CW, Proks P, Ashcroft FM, Smith PA. Electrophysiological and metabolic characterization of single β-cells and islets from diabetic GK rats. Diabetes 1998;47:73–81
47. Anello M, Lupi R, Spampinato D, Piro S, Masini M, Boggi U, Del Prato S, Rabuazzo AM, Purrello F, Marchetti P. Functional and morphological alterations of mitochondria in pancreatic beta cells from type 2 diabetic patients. Diabetologia 2005;48:282–289
48. Ihara Y, Toyokuni S, Uchida K, Odaka H, Tanaka T, Ikeda H, Hiai H, Seino Y, Yamada Y. Hyperglycemia causes oxidative stress in pancreatic β-cells of GK rats, a model of type 2 diabetes. Diabetes 1999;48:927–932
49. Sakuraba H, Mizukami H, Yagihashi N, Wada R, Hanyu C, Yagihashi S. Reduced beta-cell mass and expression of oxidative stress-related DNA damage in the islet of Japanese Type II diabetic patients. Diabetologia 2002;45:85–96
50. Del Guerra S, Lupi R, Marselli L, Masini M, Bugliani M, Sbrana S, Torri S, Pollera M, Boggi U, Mosca F, Del Prato S, Marchetti P. Functional and molecular defects of pancreatic islets in human type 2 diabetes. Diabetes 2005;54:727–735

Diabetologia (2010) 53:1472–1481
DOI 10.1007/s00125-010-1729-5

ARTICLE

Metformin suppresses hepatic gluconeogenesis and lowers fasting blood glucose levels through reactive nitrogen species in mice

Y. Fujita · M. Hosokawa · S. Fujimoto · E. Mukai · A. Abudukadier · A. Obara · M. Ogura · Y. Nakamura · K. Toyoda · K. Nagashima · Y. Seino · N. Inagaki

Received: 25 January 2010 / Accepted: 24 February 2010 / Published online: 29 March 2010

Abstract
Aims/hypothesis Metformin, the major target of which is liver, is commonly used to treat type 2 diabetes. Although metformin activates AMP-activated protein kinase (AMPK) in hepatocytes, the mechanism of activation is still not well known. To investigate AMPK activation by metformin in liver, we examined the role of reactive nitrogen species (RNS) in suppression of hepatic gluconeogenesis.
Methods To determine RNS, we performed fluorescence examination and immunocytochemical staining in mouse hepatocytes. Since metformin is a mild mitochondrial complex I inhibitor, we compared its effects on suppression of gluconeogenesis, AMPK activation and generation of the RNS peroxynitrite ($ONOO^-$) with those of rotenone, a representative complex I inhibitor. To determine whether endogenous nitric oxide production is required for $ONOO^-$ generation and metformin action, we used mice lacking endothelial nitric oxide synthase (eNOS).
Results Metformin and rotenone significantly decreased gluconeogenesis and increased phosphorylation of AMPK in wild-type mouse hepatocytes. However, unlike rotenone, metformin did not increase the AMP/ATP ratio. It did, however, increase $ONOO^-$ generation, whereas rotenone did not. Exposure of eNOS-deficient hepatocytes to metformin did not suppress gluconeogenesis, activate AMPK or increase $ONOO^-$ generation. Furthermore, metformin lowered fasting blood glucose levels in wild-type diabetic mice, but not in eNOS-deficient diabetic mice.
Conclusions/interpretation Activation of AMPK by metformin is dependent on $ONOO^-$. For metformin action in liver, intra-hepatocellular eNOS is required.

Keywords AMP · AMP-activated protein kinase · Endothelial nitric oxide synthase · Gluconeogenesis · Metformin · Nitric oxide · Peroxynitrite · Reactive nitrogen species

Abbreviations

AMPK	AMP-activated protein kinase
BAEC	Bovine aortic endothelial cells
DCDHF	2,7-Dihydrodichlorofluorescein
eNOS	Endothelial nitric oxide synthase
L-NAME	N^{ω}-Nitro-L-arginine methyl ester
NOS	Nitric oxide synthase
OCT1	Organic cation transporter 1
$ONOO^-$	Peroxynitrite
RNS	Reactive nitrogen species

Y. Fujita · M. Hosokawa (✉) · S. Fujimoto · E. Mukai · A. Abudukadier · A. Obara · M. Ogura · Y. Nakamura · K. Toyoda · K. Nagashima · Y. Seino · N. Inagaki
Department of Diabetes and Clinical Nutrition, Graduate School of Medicine, Kyoto University, 54 Shogoin, Kawahara-cho, Sakyo-ku, Kyoto 606-8507, Japan
e-mail: hosokawa@metab.kuhp.kyoto-u.ac.jp

E. Mukai
Japan Association for the Advancement of Medical Equipment, Tokyo, Japan

Y. Seino
Kansai Electric Power Hospital, Osaka, Japan

S. Fujimoto · K. Nagashima · N. Inagaki
CREST of Japan Science and Technology Cooperation (JST), Kyoto, Japan

Introduction

Metformin is one of the most commonly used oral glucose-lowering drugs for type 2 diabetes and is recommended as a first-line drug in recent treatment guidelines of the American Diabetes Association and European Association for the Study of Diabetes [1, 2]. The main target tissue of metformin is liver and its major effect is to decrease hepatic glucose output, which occurs largely due to the suppression of gluconeogenesis, leading to lower fasting blood glucose levels without insulin stimulation and weight gain [3–5]. In addition, metformin has beneficial effects on cardiovascular function and reduces cardiovascular risk in type 2 diabetes [6].

Although metformin has been used clinically for several decades, the mechanisms by which it exerts its glucose-lowering effects are still unclear [7]. Recent studies have demonstrated that therapeutic effects of metformin are mediated by activation of AMP-activated protein kinase (AMPK), leading to a decrease in gluconeogenesis and an increase of fatty acid oxidation in liver and of glucose uptake in skeletal muscle [8–10]. AMPK is a serine/threonine kinase that acts as an energy sensor and is activated in response to reductions of cellular energy levels and to environmental stress, including hypoxia, ischaemia, exercise, ATP depletion and oxidative stress [11, 12]. Although it has been known that AMPK is activated by an increase in the AMP/ATP ratio, the AMPK-activating mechanism also involves other pathways that are dependent on upstream AMPK kinases, including LKB1 kinase and calmodulin-dependent protein kinase kinase in liver and skeletal muscle, respectively [13]. Previous studies reported that metformin had an inhibitory effect on mitochondrial complex I; and, indeed, an inhibition of mitochondrial complex I has been found to increase the AMP/ATP ratio [7, 14, 15]. AMPK activation by metformin was therefore thought to be also mediated by an increase in the AMP/ATP ratio. However, recent studies have reported that metformin action may be mediated without a notable inhibition of mitochondrial metabolism [10, 16].

Recently, a possible role of peroxynitrite ($ONOO^-$), a reactive nitrogen species (RNS), in the mechanism of AMPK activation has been investigated. RNS comprises nitric oxide and its secondary substrates; $ONOO^-$ is generated from superoxide anions (O_2^-) and nitric oxide [17]. Zou et al. reported that metformin activates AMPK through $ONOO^-$ in bovine aortic endothelial cells (BAEC) [18]. However, it is unclear whether RNS generation by metformin is involved in its suppression of hepatic gluconeogenesis or whether RNS generation affects metformin's pharmacological action in lowering of fasting blood glucose levels.

To clarify the mechanism of AMPK activation in liver, we used mouse hepatocytes to investigate the involvement of the AMP/ATP ratio and RNS in AMPK activation by metformin compared with rotenone, a representative complex I inhibitor. To determine whether endogenous nitric oxide production is required for metformin action in hepatocytes, we also performed experiments using mice lacking endothelial nitric oxide synthase (eNOS) [18–21]. We demonstrated that $ONOO^-$ plays a critical role in AMPK activation by metformin in liver and that eNOS is required for metformin action in vitro and in vivo.

Methods

Animals Male C57/BL6 (wild-type) mice were obtained from Shimizu (Kyoto, Japan). Male eNOS-deficient (*eNos* [also known as *Nos3*]$^{-/-}$) mice were obtained from Jackson Laboratories (Bar Harbor, ME, USA). Mice were maintained in a temperature-controlled (25±2°C) environment with a 12 h light/dark cycle. The mice had free access to standard laboratory chow and water. All experiments were carried out with mice aged 8 to 10 weeks. The animals were maintained and used in accordance with the Guidelines for Animal Experiments of Kyoto University. All the experiments involving animals were conducted in accordance with the Guidelines for Animal Experiments of Kyoto University and were approved by the Animal Research Committee, Graduate School of Medicine, Kyoto University.

Hepatocyte preparation and culture Mice hepatocytes were isolated by collagenase digestion as described previously [22]. Primary hepatocytes were prepared by seeding in six well type 1 collagen-coated plates at a density of 1.5×10^6 cells in DMEM (low glucose, 5.6 mmol/l) containing 10% (vol./vol.) FBS, 100 nmol/l regular insulin, 50 U/ml penicillin and 50 μg/ml streptomycin. Hepatocytes were then cultured overnight in a humidified atmosphere (5% CO_2) at 37°C.

Glucose production via gluconeogenesis in hepatocytes Gluconeogenesis was measured as described previously with slight modifications [22, 23]. In brief, freshly isolated hepatocytes from mice fasted for 16 h were treated in 24 well plates (7.5×10^5 cells/well) in 0.5 ml KRB buffer (119.4 mmol/l NaCl, 3.7 mmol/l KCl, 2.7 mmol/l $CaCl_2$, 1.3 mmol/l KH_2PO_4, 1.3 mmol/l $MgSO_4$, 24.8 mmol/l $NaHCO_3$) containing 2% (wt/vol.) BSA, 2 mmol/l oleate, 0.24 mmol/l 3-isobutyl-1-methylxanthine and gluconeogenetic substrates (1 mmol/l pyruvate plus 10 mmol/l lactate) treated with metformin (Sigma, St Louis, MO, USA) and rotenone (Nacalai Tesque, Kyoto, Japan). Metformin was dissolved in water. Rotenone was dissolved in dimethyl sulfoxide to a concentration that did not interfere with cell viability (maximally 0.1% vol./vol.).

The glucose content of the supernatant fraction was measured by the glucose oxidation method using an assay kit (Gopod; Megazyme, Wicklow, Ireland). The data were normalised by protein content measured by cell lysates.

Immunoblotting analysis Freshly isolated hepatocytes were treated with metformin, rotenone and $ONOO^-$ (Dojindo, Kumamoto, Japan) in KRB buffer containing 2% (wt/vol.) BSA, 2 mmol/l oleate, 0.24 mmol/l 3-isobutyl-1-methylxanthine and gluconeogenetic substrates (1 mmol/l pyruvate plus 10 mmol/l lactate). Primary hepatocytes cultured overnight were incubated in FBS-free DMEM (no glucose) treated with metformin and rotenone. The hepatocytes were homogenised in lysis buffer (50 mmol/l Tris–HCl, pH 7.4, 50 mmol/l NaF, 1 mmol/l sodium pyrophosphate, 1 mmol/l EDTA, 1 mmol/l EGTA, 1 mmol/l dithiothreitol, 0.1 mmol/l benzamidine, 0.1 mmol/l phenylmethylsulfonylfluoride, 0.2 mmol/l sodium vanadate, 250 mmol/l mannitol, 1% (vol./vol.) Triton X-100 and 5 μg/ml soybean trypsin inhibitor). Cell lysates (50 to 150 μg protein per lane) were subjected to electrophoresis on 8% (vol./vol.) SDS–polyacrylamide gels and transferred on to nitrocellulose membranes (Protran; Schleicher and Schuell, Keene, NH, USA). Blotted membranes were incubated with each primary antibody (1:1,000 dilution). Antibodies against AMPKα and phospho-AMPKα (Thr^{172}) were from Cell Signaling Technology (Danvers, MA, USA). Antibodies against organic cation transporter 1 (OCT1) and glyceraldehyde-3-phosphate dehydrogenase were from Santa Cruz Biotechnology (Santa Cruz, CA, USA). Membranes were incubated with horseradish peroxidase-linked second antibodies (1:2,000 dilution) (GE Healthcare, Tokyo, Japan) and fluorescent bands were visualised using a western blotting detection system (Amersham ECL Plus; GE Healthcare) and then quantified by densitometry using Image J software from National Institutes of Health (Bethesda, MD, USA).

Determination of reactive nitrogen species $ONOO^-$ generation was measured using 2,7-dihydrodichlorofluorescein (DCDHF) diacetate (Cayman Chemical, Ann Arbor, MI, USA) [24–26], which is readily oxidised by $ONOO^-$ to the highly fluorescent product, dichlorofluorescein. Alone, nitric oxide, superoxide anions or hydrogen peroxide did not oxidise DCDHF. Freshly isolated hepatocytes were washed in ice-cold PBS and preloaded for 20 min at 37°C with 10 μmol/l DCDHF diacetate (Cayman Chemical) in KRB buffer containing 2% (wt/vol.) BSA, 2 mmol/l oleate, 0.24 mmol/l 3-isobutyl-1-methylxanthine and gluconeogenetic substrates (1 mmol/l pyruvate plus 10 mmol/l lactate). Fluorescence was determined using a spectrofluorophotometer (RF-5300PC; Shimazu, Kyoto, Japan) with excitation wavelength at 502 nm and emission wavelength at 523 nm. After 1 h incubation in the presence or absence of metformin, rotenone, $ONOO^-$ or hydrogen peroxide with or without RNS scavenger (5 mmol/l α-tocopherol plus 2.3 mmol/l ascorbate) [27], fluorescence was measured and presented as a ratio with respect to the value at time zero.

Immunocytochemistry Primary hepatocytes were plated on cover glass coated with 0.01% (vol./vol.) poly-L-lysine (Sigma) in six-well plates (5.0×10^5 cells per well). Hepatocytes were then incubated with FBS-free DMEM (no glucose) in the presence or absence of rotenone, metformin, metformin with RNS scavenger (5 mmol/l α-tocopherol plus 2.3 mmol/l ascorbate) and metformin with 1 mmol/l of the nitric oxide synthase (NOS) inhibitor N^{ω}-nitro-L-arginine methyl ester (L-NAME) for 2 h, or in the presence or absence of $ONOO^-$ for 5 min. The hepatocytes were fixed in 3.7% (wt/vol.) paraformaldehyde and incubated with rabbit polyclonal anti-nitrotyrosine antibody (1:100 dilution; Millipore; Billerica, MA, USA). Next, cells were incubated with goat anti-rabbit IgG fluorescein-conjugated secondary antibody (1:100 dilution; Alexa Fluor 488; Invitrogen, Carlsbad, CA, USA). Fluorescence in cells was monitored using a laser scanning microscope (LSM 510; Carl Zeiss, Tokyo, Japan) for confocal microscopy and a software package (LSM 510 Meta; Carl Zeiss) for image acquisition.

Measurement of adenine nucleotide content After freshly isolated hepatocytes were incubated in KRB buffer containing 2% (wt/vol.) BSA, 2 mmol/l oleate, 0.24 mmol/l 3-isobutyl-1-methylxanthine and gluconeogenetic substrates (1 mmol/l pyruvate plus 10 mmol/l lactate) in the presence or absence of metformin or rotenone for 2 h, or of $ONOO^-$ for 5 min, treatment was stopped by rapid addition of 0.1 ml of 2 mol/l $HClO_4$, followed by mixing by vortex and sonication in ice-cold water for 3 min. Cell lysates were then centrifuged for 3 min at 3,000×*g* and 4°C, and a fraction (0.4 ml) of the supernatant fraction was mixed with 0.1 ml of 2 mol/l HEPES and 0.1 ml of 1 mol/l Na_2CO_3. Adenine nucleotide contents were measured by a luminometric method as previously described [28, 29].

Effect of metformin on plasma glucose levels and AMPK phosphorylation in liver tissue of wild-type and $eNos^{-/-}$ diabetic mice Mice were made diabetic by intraperitoneal injection of streptozotocin (120 mg/kg) into male C57/BL6 and $eNos^{-/-}$ mice at 8 weeks of age. At 1 week after injection of streptozotocin, the animals were confirmed to be diabetic by high fed blood glucose levels (≥13.8 mmol/l) and other diabetic features, including polyuria, polydispia and hyperphagia. After fasting for 16 h, the blood glucose levels were measured and mice were immediately injected intraperitoneally with metformin (250 mg/kg) in 0.9%

sterile saline or 0.9% (wt/vol.) sterile saline only, a similar treatment to that described previously [8, 18]. Blood glucose levels were measured again after 1 h. Diabetic mice received injections of metformin or vehicle as described above for three consecutive days and blood glucose levels were measured again after fasting for 16 h. Immediately after the final measurement of blood glucose levels, the abdomen was cut open and liver tissue of each group was collected and homogenised in lysis buffer. Tissue lysates (50 μg protein/lane) were used for immunoblotting assay of AMPK phosphorylation using antibodies against AMPKα and phospho-AMPKα (Thr^{172}).

Statistical analysis Results are expressed as mean ± SE per number (n) of animals. Statistical significance was evaluated by ANOVA, unpaired t test (not noted) and paired t test (noted). A value of $p<0.05$ was considered statistically significant.

Results

Effects of metformin and rotenone on gluconeogenesis and AMPKα phosphorylation in C57/BL6 mice hepatocytes Hepatic gluconeogenesis and AMPKα phosphorylation were measured using freshly isolated hepatocytes. After 2 h exposure to metformin, hepatic gluconeogenesis was significantly and dose-dependently suppressed at doses between 0.5 and 50 mmol/l metformin; it was also suppressed by exposure to 100 nmol/l rotenone (control 115.4±2.5 nmol/mg protein, 2 mmol/l metformin 92.1±3.3 nmol/mg protein, $p<0.05$ vs control; 100 nmol/l rotenone 91.5±8.7 nmol/mg protein, $p<0.05$ vs control; Fig. 1a). Gluconeogenesis at 2 mmol/l metformin and 100 nmol/l rotenone were similar (p=NS metformin vs rotenone). After 2 h exposure, metformin (0.5–50 mmol/l) and 100 nmol/l rotenone each stimulated phosphorylation of Thr^{172} of AMPKα (Fig. 1b, c). Increments of phosphorylation relative to control in hepatocytes exposed to 2 mmol/l metformin and 100 nmol/l rotenone were almost equivalent (fold increase relative to control 1.79±0.11 [metformin] and 1.85±0.12 [rotenone], p=NS, metformin vs rotenone). Similar results were observed using primary cultured hepatocytes (Fig. 1d, e). In the time course study of exposure to 2 mmol/l metformin, the suppressing effects on gluconeogenesis appeared after 120 min ($p < 0.05$ vs corresponding control; Fig. 1f). In addition, after 60 min exposure to 2 mmol/l metformin stimulated phosphorylation of Thr^{172} of AMPKα ($p<0.05$ vs pre-exposure; Fig. 1g, h).

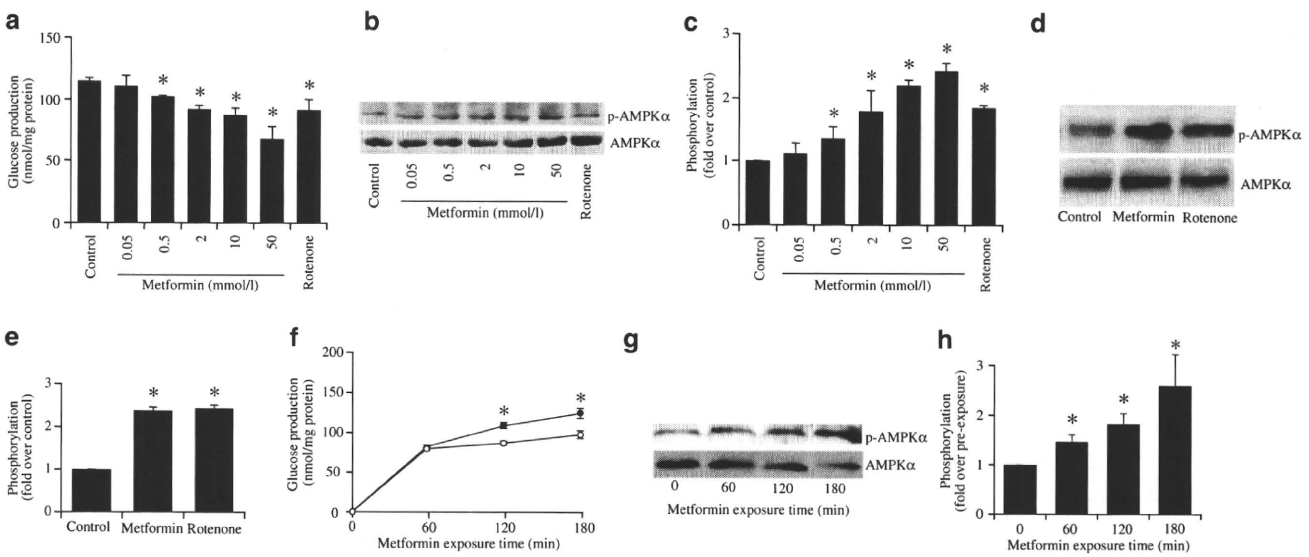

Fig. 1 Metformin and rotenone suppress gluconeogenesis and stimulate AMPKα phosphorylation in hepatocytes isolated from C57/BL6 mice. **a** Gluconeogenesis after 2 h exposure to metformin and rotenone. Metformin (dose-dependently between 0.5 and 50 mmol/l) and rotenone (100 nmol/l) significantly suppressed gluconeogenesis. **b, c** Effects of metformin and rotenone on activation of AMPK. After 2 h exposure, AMPKα phosphorylation in freshly isolated hepatocytes was significantly stimulated by metformin (dose-dependently as above [**a**]) and rotenone (100 nmol/l). Data are expressed as fold stimulation over control. **d, e** Effects of metformin and rotenone on activation of AMPK in primary cultured hepatocytes. After 2 h exposure, AMPKα phosphorylation was significantly stimulated by metformin (2 mmol/l) and rotenone (100 nmol/l). Data are expressed as fold stimulation over control. **f** Time course of gluconeogenesis with exposure to metformin. Suppressing effects on gluconeogenesis by 2 mmol/l metformin (white circles) compared with control (black circles) were detected after 120 min. **g, h** Time course of AMPK activation upon exposure to metformin (2 mmol/l), which after 60 min stimulated phosphorylation of AMPKα in freshly isolated hepatocytes. Data are expressed as fold stimulation over pre-exposure. Values (all bar graphs) are means ± SE (n=6), *$p<0.05$ vs control (**a–f**) and pre-exposure (**h**)

ATP content and AMP/ATP ratio in C57/BL6 mice hepatocytes In wild-type mice, exposure of freshly isolated hepatocytes to 100 nmol/l rotenone for 2 h decreased ATP content and increased the AMP/ATP ratio compared with control (Table 1). However, 2 h exposure to 2 mmol/l metformin did not alter ATP content or AMP/ATP ratio compared with control. ATP content and the AMP/ATP ratio at 2 mmol/l metformin and 100 nmol/l rotenone were significantly different ($p<0.01$ metformin vs rotenone).

RNS production by metformin In freshly isolated hepatocytes, exposure to 2 mmol/l metformin for 1 h increased DCDHF fluorescence, revealing an increase of $ONOO^-$ generation, whereas 300 μmol/l hydrogen peroxide or 100 nmol/l rotenone had no effect on DCDHF fluorescence (Table 2). Co-administration of RNS scavengers (vitamin E plus vitamin C) completely suppressed RNS production by metformin.

Immunocytochemical staining of primary cultured hepatocytes with anti-nitrotyrosine antibody was performed to detect $ONOO^-$ (Fig. 2). $ONOO^-$ (10 μmol/l) incubated for 5 min in primary hepatocytes increased nitrotyrosine staining. Exposure to 2 mmol/l metformin, but not to 100 nmol/l rotenone for 2 h increased nitrotyrosine staining (Fig. 2a). Similarly to the DCDHF fluorescence study, co-administration of RNS scavengers (vitamin E plus vitamin C) suppressed nitrotyrosine staining by metformin. Co-administration of L-NAME, a NOS inhibitor, suppressed $ONOO^-$ generation by metformin (Fig. 2b).

Effect of direct exposure to $ONOO^-$ on AMPKα phosphorylation and AMP/ATP ratio The direct effect of exogenous $ONOO^-$ on AMPK phosphorylation in the absence of metformin was examined. Exposure to $ONOO^-$ for 5 min stimulated phosphorylation of AMPKα by 1 to 100 μmol/l ($p < 0.05$ vs control) (Fig. 3a, b). Exposure to 10 μmol/l $ONOO^-$ for 5 min did not affect ATP content (pre-exposure 0.49±0.05 nmol/mg protein; 5 min $ONOO^-$ 0.50±0.05 nmol/mg protein, p = NS vs pre-exposure, n=5) or the AMP/ATP ratio (pre-exposure 0.99±0.06, 5 min $ONOO^-$ 0.98±0.05, p = NS vs pre-exposure, n=5).

Table 1 Effect of metformin or rotenone on ATP content and AMP/ATP ratio in hepatocytes

Treatments per mouse type	ATP (nmol/mg protein)	AMP/ATP ratio
Wild-type mice		
Control	0.45±0.08	0.98±0.07
Metformin	0.47±0.05	0.96±0.12
Rotenone	0.13±0.02**	1.94±0.13**
eNos$^{-/-}$ mice		
Control	0.42±0.07	1.22±0.11
Metformin	0.41±0.06	1.27±0.16
Rotenone	0.11±0.03**	2.34±0.23**

Values are means ± SE (n=5)

**$p<0.01$ vs control

No effect of metformin on gluconeogenesis, AMPKα phosphorylation or $ONOO^-$ generation in hepatocytes lacking eNOS In freshly isolated hepatocytes from *eNos*$^{-/-}$ mice, 2 h exposure to 2 mmol/l metformin did not suppress gluconeogenesis, whereas exposure to 100 nmol/l rotenone suppressed gluconeogenesis to a similar degree to that observed in wild-type hepatocytes (control 110.1± 4.4 nmol/mg protein, metformin 107.0±3.9 nmol/mg protein, p=NS vs control; rotenone 81.6±8.8 nmol/mg protein, $p<0.05$ vs control; Fig. 4a). Metformin did not stimulate AMPKα phosphorylation in freshly isolated hepatocytes from *eNos*$^{-/-}$ mice, whereas rotenone significantly stimulated AMPKα phosphorylation (fold increase relative to control at 2 h: metformin 0.96±0.12, p=NS vs control; rotenone 1.94±0.13, $p<0.05$ vs control; Fig. 4b, c). Similarly, in primary cultured hepatocytes, metformin also did not stimulate, whereas rotenone significantly stimulated AMPKα phosphorylation (Fig. 4d, e). Metformin also did not increase nitrotyrosine staining in primary cultured hepatocytes from *eNos*$^{-/-}$ mice, indicating no generation of $ONOO^-$ (Fig. 4f). In addition, nitrotyrosine staining was not induced by 2 h exposure to rotenone. Exposure of *eNos*$^{-/-}$ freshly isolated hepatocytes to 100 nmol/l rotenone also decreased ATP content and increased the AMP/ATP ratio, whereas exposure to metformin had not effect (Table 1). Recently, it was reported that metformin is first transported across the plasma membrane before exerting its cellular action, a step mediated by OCT1 [30]. To exclude involvement of OCT1 in *eNos*$^{-/-}$ mice, we confirmed that levels of OCT1 protein in freshly isolated hepatocytes from *eNos*$^{-/-}$ mice were similar to those in wild-type mice hepatocytes (Fig. 4g).

Essential role of eNOS in lowering of glucose levels by metformin in diabetic mice in vivo To determine whether metformin lowers fasting blood glucose levels in the absence of eNOS, metformin (250 mg/kg) was injected intraperitoneally into streptozotocin-induced diabetic wild-type or *eNos*$^{-/-}$ mice. Characteristics of wild-type and *eNos*$^{-/-}$ mice used in the experiments showed no significant differences in body weight, fasting blood glucose levels or fed blood glucose levels before streptozotocin injection at 8 weeks of age among the four groups (Table 3).

Fasting blood glucose levels were lowered by about 3.9 mmol/l at 1 h after single administration of metformin in overnight-fasted wild-type diabetic mice, whereas those in overnight-fasted *eNos*$^{-/-}$ diabetic mice were not altered

Table 2 Effect of metformin on RNS production

Treatments	No addition	Addition of vitamins E and C
Control	1.03±0.01	0.94±0.01**
Metformin (2 mmol/l)	1.15±0.04*	0.95±0.01**
Rotenone (100 nmol/l)	1.03±0.02	0.99±0.01**
Hydrogen peroxide (300 μmol/l)	1.02±0.02	0.98±0.01**
$ONOO^-$ (10 μmol/l)	1.21±0.05*	1.00±0.01**

Data are expressed as the value at 60 min divided by the value at time zero (fold increase); values are means ± SE (n=8)

*p<0.05 vs control; **p<0.01 vs corresponding values without RNS scavengers

(Table 3). Administration of vehicle (saline) alone in overnight-fasted wild-type diabetic mice did not alter fasting blood glucose levels after single administration, as was also found in overnight-fasted *eNos*$^{-/-}$ diabetic mice (Table 3). Following the first injection, daily administration of metformin was continued for two more days. Administration of metformin for three consecutive days lowered fasting blood glucose levels by about 7.1 mmol/l in wild-type diabetic mice, whereas it had no lowering effect on fasting blood glucose in diabetic *eNos*$^{-/-}$ mice (Table 3). Administration of vehicle (saline) alone in overnight-fasted wild-type mice did not alter fasting blood glucose levels after administration for three consecutive days, as was also the case in *eNos*$^{-/-}$ mice (Table 3).

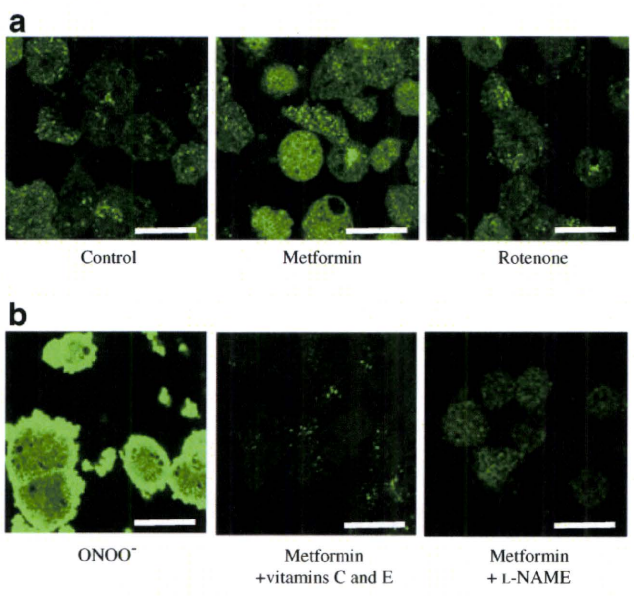

Fig. 2 Immunocytochemical staining with anti-nitrotyrosine antibody for detection of $ONOO^-$ generation. $ONOO^-$ (10 μmol/l) incubated for 5 min was used as a positive control. **a** Exposure to metformin (2 mmol/l) for 2 h increased staining, but exposure to rotenone (100 nmol/l) for the same time did not. **b** $ONOO^-$ generation induced by metformin was decreased by co-administration with RNS scavengers (5 mmol/l α-tocopherol [vitamin E] plus 2.3 mmol/l ascorbate [vitamin C]) and a NOS inhibitor (1 mmol/l L-NAME), respectively. Confocal microscopy, magnifications ×100; scale bars 50 μm

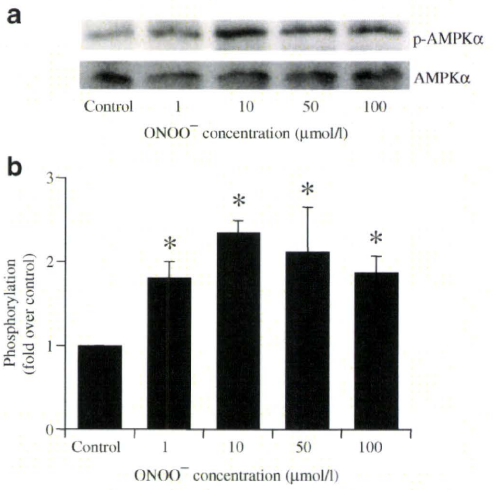

Fig. 3 Exogenous $ONOO^-$ stimulates AMPKα phosphorylation in freshly isolated hepatocytes. **a** Blot showing that direct exposure to $ONOO^-$ for 5 min at doses ranging from 1 to 100 μmol/l stimulated AMPKα phosphorylation. **b** Quantification with data expressed as fold stimulation over control. Values are means ± SE (n=4), *p<0.05 vs control

Lack of effects of metformin in vivo on AMPKα phosphorylation in liver tissues lacking eNOS In liver tissue samples collected after three consecutive days of administration, metformin stimulated phosphorylation of AMPKα in wild-type mice (metformin 2.17±0.30 [fold increase relative to vehicle], p<0.05 vs vehicle; Fig. 5a, b). However, stimulation of AMPKα phosphorylation by metformin was not observed in liver tissues of *eNos*$^{-/-}$ mice (metformin 0.97±0.12 [fold increase relative to vehicle], p=NS vs saline; Fig. 5a, c).

Discussion

In the present study, we show for the first time that activation of AMPK and the inhibitory effect on hepatic gluconeogenesis by metformin are mediated by generation of the RNS, $ONOO^-$. We also showed that eNOS plays an important role in metformin action in liver.

We investigated the metformin–RNS–AMPK pathway for its suppressing effects on hepatic gluconeogenesis. Because recent studies have shown that metformin activates AMPK through the RNS, $ONOO^-$, in BAEC [18], we evaluated RNS production in liver, the major target of metformin action. We found that metformin increased $ONOO^-$ generation and that $ONOO^-$ itself activates AMPK, which is induced in only 5 min. A previous study found that AMPK phosphorylation by metformin does not appear within 10 min but only after 30 min [31]. Consistent

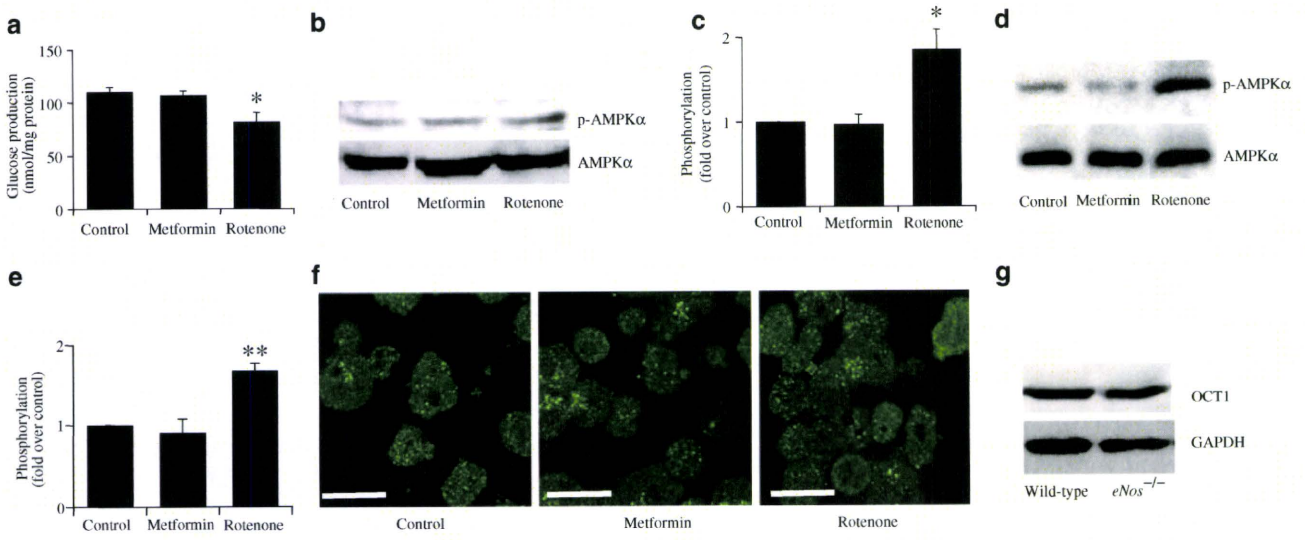

Fig. 4 Lack of effects of metformin on suppression of gluconeogenesis, AMPKα phosphorylation and $ONOO^-$ generation in hepatocytes lacking eNOS. **a** Metformin (2 mmol/l) did not suppress gluconeogenesis after 2 h exposure in hepatocytes lacking eNOS, but rotenone (100 nmol/l) suppressed gluconeogenesis to a similar degree to that observed in wild-type hepatocytes. Values are means ± SE (n=6), *p< 0.05 vs control. **b** Blot showing that AMPKα phosphorylation was not stimulated by metformin (2 mmol/l), but was stimulated by rotenone (100 nmol/l) after 2 h exposure in freshly isolated hepatocytes; (**c**) quantification with data expressed as fold stimulation over control. Values are means ± SE (n=4), *p<0.05 vs control. **d** Blot showing that AMPKα phosphorylation was not stimulated by metformin (2 mmol/l), but was stimulated by rotenone (100 nmol/l) after 2 h exposure in primary cultured hepatocytes, with (**e**) bar graph showing data expressed as fold stimulation over control. Values are means ± SE (n=5), **p<0.01 vs control. **f** Immunocytochemical staining (confocal microscopy) with anti-nitrotyrosine antibody in hepatocytes lacking eNOS. Exposure to metformin (2 mmol/l) and rotenone (100 nmol/l) for 2 h did not increase staining. Magnification ×100, scale bar 50 μm. **g** Levels of OCT1 protein in wild-type and *eNos*$^{-/-}$ mice hepatocytes. OCT1 levels in *eNos*$^{-/-}$ mice hepatocytes were similar to those in wild-type mice hepatocytes. Findings normalised to glyceraldehyde-3-phosphate dehydrogenase (GAPDH)

with that study, our data showed that AMPK phosphorylation by metformin did not appear within 15 min, but only after more than 30 min (data not shown). Thus, $ONOO^-$ generation appears to precede AMPK phosphorylation after exposure to metformin. $ONOO^-$ is generated by nitric oxide and superoxide anions; intra-hepatocellular nitric oxide is produced by NOS. In the present study, the NOS inhibitor, L-NAME, suppressed $ONOO^-$ production by metformin. This suggests that nitric oxide production by hepatocellular NOS is required for $ONOO^-$ production by metformin. Since eNOS is the representative subtype of the NOS family for generation of $ONOO^-$ in liver [17], we sought to determine whether eNOS is required for $ONOO^-$ production by metformin. Using eNOS-deficient mice, we were able to demonstrate that eNOS is essential for metformin action in liver. Thus metformin increases $ONOO^-$ produc-

Table 3 Effect of metformin on blood glucose levels in wild-type and *eNos*$^{-/-}$ diabetic mice

Treatments per mouse type	Pre streptozotocin			Post streptozotocin		
	Body weight (g)	FBG (mmol/l)	Fed BG (mmol/l)	FBG (mmol/l)	BG (mmol/l) at 1 h PM	FBG (mmol/l) after 3 days met
Wild-type mice						
Saline	20.3±0.4	3.7±0.2	8.2±0.5	16.0±2.7	17.2±3.1	16.6±3.3
Metformin	20.4±0.3	3.7±0.2	8.0±0.3	16.6±2.8	12.7±3.0**	9.5±1.9**
eNos$^{-/-}$ mice						
Saline	20.5±0.3	3.6±0.2	7.9±0.4	15.0±1.9	17.3±2.4	16.9±2.7
Metformin	20.7±0.3	3.5±0.2	8.1±0.5	15.8±1.6	19.0±1.9	16.5±2.1

Values are means ± SE (n=8)

**p<0.01 vs the value of pre-injection intraperitoneally with metformin in saline or saline only, paired t test

BG, blood glucose; FBG, fasting blood glucose; met, metformin; PM, post-metformin

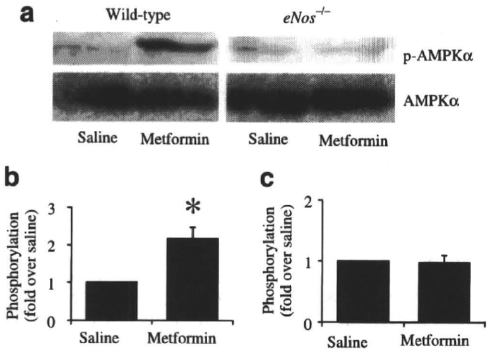

Fig. 5 Lack of effects of metformin in vivo on AMPKα phosphorylation in liver tissues deficient in eNOS. **a** Blot showing that metformin stimulated phosphorylation of AMPKα in liver tissues of wild-type diabetic mice after administration for three consecutive days. **b** Quantification of blot for wild-type and (**c**) *eNos*$^{-/-}$ mice. Metformin did not stimulate (**a**, **c**) phosphorylation of AMPKα in liver tissues of *eNos*$^{-/-}$ diabetic mice after metformin administration for three consecutive days. Data (**b**, **c**) are expressed as fold stimulation over saline. Values are means ± SE (n=5), *p<0.05 vs vehicle

tion, which is followed by AMPK activation and suppression of gluconeogenesis.

Although metformin has been reported not to affect the ATP content of hepatocytes [32], several studies have found that metformin decreased ATP content and/or increased the AMP/ATP ratio in hepatocytes [23, 33], possibly a result of metformin's suppressive effect on complex I activity in the respiratory chain [34] and one that plays an important role in AMPK activation by metformin. While metformin was found not to affect ATP content and the AMP/ATP ratio in the present study, the AMP/ATP ratio might nevertheless play an important role in AMPK activation by metformin because AMPK is sensitive to changes in the AMP/ATP ratio at levels too slight to be detected by measurement of the total adenine nucleotide content of whole cells [35]. Interestingly, metformin activates AMPK with a smaller increase in the AMP/ATP ratio than that effected by mitochondrial uncoupler and rosiglitazone [16] and without affecting the ADP/ATP ratio [10]. These results suggest that, apart from increases in the AMP/ATP ratio, other important mechanisms may be involved in AMP activation by metformin.

Rotenone inhibits complex I of the mitochondrial respiratory chain and decreases oxidative phosphorylation, leading to ATP depletion and an increase in the AMP/ATP ratio, which results in stimulation of AMPK phosphorylation. In the present study we observed that while 2 mmol/l metformin and 100 nmol/l rotenone had similar effects on gluconeogenesis and AMPK phosphorylation, the AMP/ATP ratio increased prominently only upon exposure to rotenone but not upon exposure to metformin. These results indicate that complex I inhibition alone is unlikely to explain the action of metformin. Interestingly, metformin significantly increased RNS in contrast to the lack of effect of rotenone on RNS. Furthermore, a decrease in metformin-induced RNS production by eNOS disruption abolished activation of AMPK by metformin. These results demonstrate that RNS is a regulator distinct from the AMP/ATP ratio in AMPK activation by metformin.

Some groups have reported that eNOS acts upstream of AMPK activation in BAEC [18], while other groups have reported that eNOS acts downstream of AMPK activation in capillary endothelial cells and in cardiomyocytes [21]. In the present study, we show that, in wild-type hepatocytes, direct exposure to $ONOO^-$ activates AMPK and that rotenone activates AMPK without increase in $ONOO^-$ production, supporting the former notion [18] in hepatocytes.

It is well known that high levels of RNS have deleterious effects on cell function and viability [17]. On the other hand, the low levels of RNS seen in physiological conditions are required for maintaining normal cell functions such as signal transduction [36]. For example, it has been reported that RNS production induced by skeletal muscle contraction is correlated with glucose uptake [20]. Thus, RNS has protective and damaging effects on cells. Indeed, the RNS produced by metformin at a dose used in the present study (2 mmol/l) should have beneficial effects on hepatic glucose metabolism through AMPK activation.

We demonstrate in the present study that AMPK activation by metformin in hepatocytes is dependent on RNS. We also demonstrate that eNOS plays an important role in suppressing hepatic gluconeogenesis in vitro as well as in lowering fasting blood glucose levels in vivo. It is generally accepted that fasting blood glucose levels are determined by hepatic gluconeogenesis, which suggests that eNOS is required for metformin's action on fasting blood glucose levels.

In the present study, we have elucidated a novel mechanism for metformin action. However, some limitations of this study must be considered. In our in vivo metformin experiments, the mice were injected intraperitoneally with 250 mg/kg metformin in 0.9% sterile saline, which is a similar dosage to that used previously [8, 18]. This protocol using a high dose of metformin for rodents may cause a very distinct acute response. Therefore, we cannot exclude the possibility that the acute hepatocellular response to AMPK activation by metformin in the present study differs from the clinical effects of metformin when used to treat patients with type 2 diabetes. To elucidate the detailed mechanisms of AMPK activation by metformin in liver, which may provide novel therapeutic targets for type 2 diabetes, further investigations are required.

Acknowledgements This study was supported by Scientific Research Grants, a Grant for Leading Project for Biosimulation from the Ministry of Education, Culture, Sports, Science and Technology of Japan, and by a grant from CREST of Japan Science and Technology Cooperation. Support was also provided in the form of a grant from the Ministry of Health, Labor and Welfare, Japan, and also by Kyoto University Global COE Program 'Center for Frontier Medicine'.

Duality of interest The authors declare that there is no duality of interest associated with this manuscript.

References

1. Nathan DM, Buse JB, Davidson MB et al (2008) Management of hyperglycaemia in type 2 diabetes mellitus: a consensus algorithm for the initiation and adjustment of therapy. Update regarding the thiazolidinediones. Diabetologia 51:8–11
2. Nathan DM, Buse JB, Davidson MB et al (2006) Management of hyperglycaemia in type 2 diabetes: a consensus algorithm for the initiation and adjustment of therapy. A consensus statement from the American Diabetes Association and the European Association for the Study of Diabetes. Diabetologia 49:1711–1721
3. Inzucchi SE, Maggs DG, Spollett GR et al (1998) Efficacy and metabolic effects of metformin and troglitazone in type II diabetes mellitus. N Engl J Med 338:867–873
4. Scarpello JH, Howlett HC (2008) Metformin therapy and clinical uses. Diab Vasc Dis Res 5:157–167
5. Bailey CJ (1992) Biguanides and NIDDM. Diabetes Care 15:755–772
6. UK Prospective Diabetes Study (UKPDS) Group (1998) Effect of intensive blood-glucose control with metformin on complications in overweight patients with type 2 diabetes (UKPDS 34). Lancet 352:854–865
7. Brunmair B, Staniek K, Gras F et al (2004) Thiazolidinediones, like metformin, inhibit respiratory complex I. Diabetes 53:1052–1059
8. Shaw RJ, Lamia KA, Vasquez D et al (2005) The kinase LKB1 mediates glucose homeostasis in liver and therapeutic effects of metformin. Science 310:1642–1646
9. Zhou G, Myers R, Li Y, Chen Y et al (2001) Role of AMP-activated protein kinase in mechanism of metformin action. J Clin Invest 108:1167–1174
10. Hawley SA, Gadalla AE, Olsen GS, Hardie DG (2002) The antidiabetic drug metformin activates the AMP-activated protein kinase cascade via an adenine nucleotide-independent mechanism. Diabetes 51:2420–2425
11. Tian R, Musi N, D'Agostino J, Hirshman MF, Goodyear LJ (2001) Increased adenosine monophosphate-activated protein kinase activity in rat hearts with pressure-overload hypertrophy. Circulation 104:1664–1669
12. Hardie DG (2004) The AMP-activated protein kinase pathway—new players upstream and downstream. J Cell Sci 117:5479–5487
13. Hardie DG, Hawley SA, Scott JW (2006) AMP-activated protein kinase—development of the energy sensor concept. J Physiol 574: 7–15
14. El-Mir MY, Nogueira V, Fontaine E, Ave'ret N, Rigoulet M, Leverve X (2000) Dimethylbiguanide inhibits cell respiration via an indirect effect targeted on the respiratory chain complex I. J Biol Chem 275:223–228
15. Owen MR, Doran E, Halestrap AP (2000) Evidence that metformin exerts its anti-diabetic effects through inhibition of complex 1 of the mitochondrial respiratory chain. Biochem J 348:607–614
16. Fryer LG, Parbu-Patel A, Carling D (2002) The anti-diabetic drugs rosiglitazone and metformin stimulate AMP-activated protein kinase through distinct signaling pathways. J Biol Chem 277:25226–25232
17. Pacher P, Beckman JS, Liaudet L (2007) Nitric oxide and $ONOO^-$ in health and disease. Physiol Rev 87:315–424
18. Zou MH, Kirkpatrick SS, Davis BJ et al (2004) Activation of the AMP-activated protein kinase by the anti-diabetic drug metformin in vivo. Role of mitochondrial reactive nitrogen species. J Biol Chem 279:43940–43951
19. Davis BJ, Xie Z, Viollet B, Zou MH (2006) Activation of the AMP-activated kinase by antidiabetes drug metformin stimulates nitric oxide synthesis in vivo by promoting the association of heat shock protein 90 and endothelial nitric oxide synthase. Diabetes 55:496–505
20. Ross RM, Wadley GD, Clark MG, Rattigan S, McConell GK (2007) Local nitric oxide synthase inhibition reduces skeletal muscle glucose uptake but not capillary blood flow during in situ muscle contraction in rats. Diabetes 56:2885–2892
21. Chen ZP, Mitchelhill KI, Michell BJ et al (1999) AMP-activated protein kinase phosphorylation of endothelial NO synthase. FEBS Lett 443:285–289
22. Fujiwara H, Hosokawa M, Zhou X et al (2008) Curcumin inhibits glucose production in isolated mice hepatocytes. Diabetes Res Clin Pract 80:185–191
23. Argaud D, Roth H, Wiernsperger N, Leverve XM (1993) Metformin decreases gluconeogenesis by enhancing the pyruvate kinase flux in isolated rat hepatocytes. Eur J Biochem 213:1341–1348
24. Kooy NW, Royall JA, Ischiropoulos H (1997) Oxidation of 2′,7′-dichlorofluorescin by $ONOO^-$. Free Radic Res 27:245–254
25. Crow JP (1997) Dichlorodihydrofluorescein and dihydrorhodamine 123 are sensitive indicators of $ONOO^-$ in vitro: implications for intracellular measurement of reactive nitrogen and oxygen species. Nitric Oxide 2:145–157
26. Possel H, Noack H, Augustin W, Keilhoff G, Wolf G (1997) 2,7-Dihydrodichlorofluorescein diacetate as a fluorescent marker for $ONOO^-$ formation. FEBS Lett 416:175–178
27. Kominato R, Fujimoto S, Mukai E et al (2008) Src activation generates reactive oxygen species and impairs metabolism-secretion coupling in diabetic Goto–Kakizaki and ouabain-treated rat pancreatic islets. Diabetologia 51:1226–1235
28. Nabe K, Fujimoto S, Shimodahira M et al (2006) Diphenylhydantoin suppresses glucose-induced insulin release by decreasing cytoplasmic H^+ concentration in pancreatic islets. Endocrinology 147:2717–2727
29. Fujimoto S, Mukai E, Hamamoto Y et al (2002) Prior exposure to high glucose augments depolarization-induced insulin release by mitigating the decline of ATP level in rat islets. Endocrinology 143:213–221
30. Shu Y, Sheardown SA, Brown C et al (2007) Effect of genetic variation in the organic cation transporter 1 (OCT1) on metformin action. J Clin Invest 117:1422–1431
31. Xie Z, Dong Y, Scholz R, Neumann D, Zou MH (2008) Phosphorylation of LKB1 at serine 428 by protein kinase C-ζ is required for metformin-enhanced activation of the AMP-activated protein kinase in endothelial cells. Circulation 117: 952–962
32. Wollen N, Bailey CJ (1988) Inhibition of hepatic gluconeogenesis by metformin. Synergism with insulin. Biochem Pharmacol 37:4353–4358
33. Guigas B, Bertrand L, Taleux N et al (2006) 5-Aminoimidazole-4-carboxamide-1-beta-D-ribofuranoside and metformin inhibit